NIS-ACT
NIS-P

Effects of assumed changes in the Near Ultraviolet Radiation on the Photochemical Distribution of Atmospheric Ozone and on the Heating Rates in the Stratosphere*

S. I. Rasool
Goddard Institute for Space Studies
National Aeronautics and Space Administration
New York 27, New York

*Presented at the XIII General Assembly of IUGG, Berkeley, California, August 19-31, 1963.

(NASA-TM-101924) EFFECTS OF ASSUMED CHANGES IN THE NEAR ULTRAVIOLET RADIATION ON THE PHOTOCHEMICAL DISTRIBUTION OF ATMOSPHERIC OZONE AND ON THE HEATING RATES IN THE STRATOSPHERE (NASA) 51 p
N90-71248
Unclas
00/45 0277431

I. Introduction

An experiment has recently been proposed (Rasool 1961, Appendix I) in which a filter apparatus is to be flown on a Nimbus series of satellites with a view of detecting time variations, if any, in the intensity of the near ultraviolet radiation from the sun. The experiment is concerned with the spectral intervals of 1700 - 2300 Å and 2300 - 3000 Å, being the regions which control the photo-chemical equilibrium of the atmospheric ozone and the thermal balance of the earth's stratosphere.

In order to demonstrate the geophysical significance of such an experiment, the following calculations have been made which show the effect of assumed changes in the intensity of near ultraviolet radiation on the structure of the earth's stratosphere. Vertical distribution of atmospheric ozone and the heating rates in the stratosphere have been computed for nine different cases in which the near ultraviolet radiation

intensity is assumed to change both uniformly and differentially by $\pm$ 50%. This range of variation in the radiation intensity of the near ultraviolet is within the limits of the scatter in the solar radiation data so far available in the literature (Fig. 1). The results show that at altitudes > 30 km, both the ozone distribution and the heating rates are very sensitive to these changes. At the altitude of 60-70 km, the ozone concentration may change by more than a factor of 2 and the heating rates by $\sim 8^{\circ}$ K/day. The changes in the total ozone amount are, however, smaller than the day to day variations normally observed in the middle latitudes.

The importance of the reaction rate values adopted for the calculations of the photochemical distribution of atmospheric ozone is stressed in Appendix II. The extreme values for the reaction rates,

K_1 $(O + O + M \longrightarrow O_2 + M)$ and K_2 $(O + O_2 + M \longrightarrow O_3 + M)$

quoted in the literature differ by a factor of 20.

Though for the main calculations we have adopted the most recent and supposedly the most reliable values for K_1 and K_2, calculations have also been repeated for four other

cases where different combinations for K_1 and K_2 values have been adopted. The results are given in Appendix II which show the extreme sensitivity of the calculated ozone distributions and the heating rates in the upper stratosphere and the mesosphere to the changes in value of K_1 and K_2.

II. Geophysical importance of the near ultraviolet radiation from the sun

The solar radiation in the near ultraviolet (1700-3000 Å) is absorbed by the earth's atmosphere at an altitude between 30 and 70 km and is responsible for the formation of the ozone layer at that altitude (Fig. 2, Curve 2).

Molecular oxygen is dissociated into atomic oxygen by the radiation of wavelengths less than 2450 Å. The atomic oxygen thus produced combines with molecular oxygen to produce ozone, which in turn is itself dissociated into atomic and molecular oxygen mainly by the action of solar radiation contained in the wavelength interval 2200-3000 Å.

The following photochemical reactions principally govern the equilibrium of the ozone layer in the earth's atmosphere:

$$O_2 + h\nu \ (< 2450\ \text{Å}) \longrightarrow O + O \qquad (1)$$

$$O + O + M \xrightarrow{K_1} O_2 + M \qquad (2)$$

$$O + O_2 + M \xrightarrow{K_2} O_3 + M \qquad (3)$$

$$O_3 + h\nu \ (< 11000\ \text{Å}) \longrightarrow O_2 + O \qquad (4)$$

$$O_3 + O \xrightarrow{k_3} 2O_2 \qquad (5)$$

where $h\nu$ represents the photo-energy required to dissociate an oxygen or ozone molecule, K_1, K_2 and K_3 are the rate coefficients for the reactions (2), (3), and (5), and M is the third body in the three-body collision processes (2) and (3). The presence of a third body which may be a molecule of nitrogen or oxygen or even an atom of oxygen is necessary to preserve the total energy and momentum of the particles involved in the recombination.

In these processes of dissociation and recombination a significant amount of energy is deposited at these altitudes which, on an average, raises the temperature of the middle atmosphere to a maximum value of $\sim 270^{\circ}$ K at 50 km (Fig. 3). This particular type of temperature profile makes the atmospheric region between 20 and 50 km altitude very stable against

convection, but the circulation patterns in this region are to some extent related to geographical, seasonal and short-period variations in this temperature profile. (Teweles 1961)

Recent rocket measurements by Stroud et al. (1960) show significant day to day variations in the temperature structure of the upper stratosphere and the mesosphere. Moreover, there is also some evidence of geographical and seasonal changes (Nordberg 1962) (Israel 1962).

No generally accepted explanation is so far available to account for these variations. One of the main reasons for this discrepancy is the lack of knowledge about the time variations in the intensity of the near ultraviolet radiation which is the main source of heating at these altitudes.

The following caluclations of the photochemical distribution of ozone and the heating rates in the stratosphere and the mesosphere will show the significance of radiation changes on these parameters.

III. Photochemical distribution of ozone

From the five reactions mentioned above, the equilibrium ozone concentration at any level can be expressed as follows (Dütsch 1961):

$$n_3 = n_2 \left[\frac{(f_2/f_3)(k_2/k_3)\, n\, n_2}{f_3 (k_1/k_2 k_3) + n_2} \right]^{1/2}$$

where n_1, n_2, n_3 are the number densities of the air molecules, molecular oxygen and ozone respectively; f_2 and f_3 are the number of quanta absorbed per molecule per unit time :

$$f_2 = \int_\lambda \sigma_2 q_{(\lambda)} d\lambda = \int_\lambda \sigma_2 q_\infty(\lambda)\, e^{-(\sigma_2 N_2 + \sigma_3 N_3)}\, d\lambda$$

$$f_3 = \int_\lambda \sigma_3 q_{(\lambda)} d\lambda = \int_\lambda \sigma_2 q_\infty(\lambda)\, e^{-(\sigma_2 N_2 + \sigma_3 N_3)}\, d\lambda$$

σ_2 and σ_3 are the absorption cross section of O_2 and O_3 respectively; $q_\infty(\lambda)$ is the number of quanta /cm^2/sec/Å available at the top of the atmosphere; N_2 and N_3 represent the total number of oxygen and ozone molecules above the level z in the direction of the solar beam.

$$N_2 = \int_z^\infty n_2 dz \sec\theta \qquad \text{and} \qquad N_3 = \int_z^\infty n_3 dz \sec\theta$$

where θ is the zenith angle of the sun.

K_1, K_2 and K_3 are the rates of reaction (2), (3) and (5) and will be discussed in greater detail in a later section.

Calculations of the photochemical distribution of ozone were made using the following values of each of the above mentioned parameters:

(i) Vertical distribution of temperature and density in the earth's atmosphere

Figures (3) and (4) show the temperature and density variation with altitude recently reported by Nordberg and Stroud (1961). These are based on the rocket measurements made at Guam in 1958. We have assumed that these profiles are characteristic of a tropical atmosphere and have adopted them for our calculations.

(ii) Spectral distribution of solar radiation

Figure (1) gives a summary of the up-to-date measurements of the intensity of the solar flux made by rockets in the past several years. Also given are the values which have been deduced theoretically by Allen (1958). These last values have been mainly used so far by many authors to calculate the photochemical distribution of ozone. From the figure it is clear, particularly in the region of 2200 Å, that the uncertainty is of the order of a factor of two.

For our calculations of the photochemical distribution of ozone, the solar spectrum has been arbitrarily divided into three parts: 1700-2300 Å (Q_1), 2300-3000 Å (Q_2), and 3000-7800 Å. For Q_1 we assume a spectral distribution of energy which lies between the values given by Detwiler et al. (1961) and Allen (1958). For Q_2 we adopt the curve given by Johnson et al (1954). In the visible region it is assumed that the sun radiates as a black body at a temperature of 5740 ^{o}K. This spectral distribution of energy is used to calculate a mean ozone distribution (hitherto referred to as 'normal' case). Q_1 and Q_2 are now allowed to vary by ±50%, both uniformly and differentially, which give eight other types of energy distributions in the near ultraviolet. Ozone calculations are repeated for each of these cases.

(iii) Absorption cross sections for ozone and oxygen

Figure 5 shows the absorption cross sections employed in these calculations for the near ultraviolet region. The oxygen absorption cross sections in the spectral interval 1700-2200 Å have been taken from Watanabe (1958) and, for

spectral regions $>$ 2200 Å, from London, Ooyama and Prabhakara (1962).

In the spectral region from 2300 to 3000 Å, the absorption coefficient values for ozone adopted here are those due to Vigroux (1952). For wavelengths $<$ 2300 Å the values shown in the figure are taken from Inn and Tanaka (1956). Absorption coefficients of ozone in the visible region (Chappuis band) have been adopted from Vigroux (1952).

(iv) Rate coefficients

During the past few years, due to more and more experimentation in this field, the values of the rate coefficients for the reactions 2, 3, and 5 have become much more uncertain. The extreme values quoted in the literature for the same temperature differ by a factor of 20. Recently, however, Kaufman and Kelso (1961) have made some very careful measurements of K_1 and K_2 in the laboratory, and have given the following values, which are now assumed to be most reliable:

$$K_1 = 3 \times 10^{-33} \text{ cm}^6/\text{molecule}^2/\text{sec}$$

$$K_2 = 1.2 \times 10^{-34} \text{ cm}^6/\text{molecule}^2/\text{sec}$$

We have used these values of k_1 and k_2 in our calculations, but as no recent estimate for k_3 was available, the values of k_3 have been taken from the results given by Campbell and Nudelmann (1960). The reaction rate coefficient values for k_1 and k_2 have been assumed to be temperature independent, while for k_3 the following temperature dependence was adopted:

$$k_3 = 5.44 \times 10^{12} \exp\left[-2133/T\right] \quad cm^3/gm\ mol/sec$$

Using the above mentioned numerical values for the various parameters in equation (1), the vertical distributions of ozone for the nine different cases were calculated by programming the computation for an IBM 7090.

The atmosphere between 10-75 km was divided into 26 layers, each 2.5 km thick. It was assumed that above 75 km the ozone concentration decreased with altitude with a scale height of 8 km. Above 90 km, however, the ozone amount was assumed to be zero.

Due to rapid photodissociation of molecular oxygen at altitudes $\gtrsim$ 75 km, it was assumed that above 75 km the density of molecular oxygen decreases with height much more

rapidly, with a scale height of 6 km. This assumption will imply that at 150 km the density of molecular oxygen has decreased to $\sim 10^9$ particles/cc (compared to 10^{14}/cc at 75 km). This is compatible with recent results reported by Hinteregger (1962).

The computations were programmed in such a way that the mean ozone amount in each layer was determined by iteration, taking into account the depletion of the solar radiation within the layer as well.

Results

The results of these computations are shown in Figures 2 (curve 1), 6a, 7a, 8a, and 9a.

Figure 2 (curve 1) shows the calculated ozone distribution in the earth's atmosphere for the 'normal' case in which the mean values of solar intensities in the near ultraviolet were used for the calculations. In the same figure is also drawn the observed profile of ozone distribution in the earth's atmosphere for equatorial regions (curve 2) (Paetzold 1956). A comparison of the two curves indicates a reasonably good agreement between the calculated and observed ozone distributions.

Figures 6a, 7a, 8a, and 9a show the ozone distributions obtained for eight different cases when the solar flux in the Q_1 and Q_2 regions have been allowed to vary by $\pm$ 50%. In each figure, the solid line curve has been reproduced which represents the 'normal' case.

It is interesting to notice that 1) a change in the solar radiation intensity in the near ultraviolet affects the photochemical distribution of ozone only above 25 km altitude, 2) the maximum change of about a factor of 2 in the ozone concentration takes place when Q_1 and Q_2 vary in opposite directions by 50%, (Figure 9a), and 3) a uniform change in intensity by plus or minus 50% over the whole spectral region of 1700-3000 Å does not seem to affect the ozone distribution to any significant degree, (Figure 8a).

The other cases show small amount of changes in the ozone distributions in the right direction when only Q_1 or Q_2 are increased or decreased by 50%.

Heating rates

For each of the above mentioned nine cases, calculations have also been made of the heating rates due to the absorption

of radiation by ozone and oxygen.

The heating in any layer is given by the absorption per unit mass.

$$H_{(z)}\ {}^{\circ}K/day = \int_{t} \frac{E(z)}{\rho_{(z)} C_p}\, dt$$

where $E(z)$ is the amount of energy in erg/cm^3/sec deposited in any layer at level z, ρ is the average density of the layer in gm/cm^3, and C_p is the specific heat at constant pressure. The expression is numerically integrated over a 12 hour day by computing the energy deposited every hour for varying solar zenith angles. The mean declination of the sun was assumed to be 15°, which was supposed to give an average of the year for the equator.

Figures 6b, 7b, 8b, and 9b show the variation of heating rates with height for the same nine cases. As before, the solid line curve in each figure represents the 'normal' case.

It is interesting to note that for the normal case the maximum heating rates of 16 $^{\circ}$K/day are achieved at the altitude of $\sim$ 62 km, and that there is a secondary maximum of 13 $^{\circ}$K/day at $\sim$ 45 km. Our values up to 45 km agree very well with those recently published by London et al. (1962) for equatorial regions.

For altitudes higher than 45 km, the results of these authors, however, show that the heating rates continue to increase up to 80 km. As pointed out by London et al, the heating rates at higher altitudes are extremely sensitive to the ozone concentrations at these altitudes, which in turn are very much influenced by the values of k_1 and k_2 adopted for the calculations.

In Appendix II the importance of k_1 and k_2 values in the calculations of the ozone distribution and the heating rates have been discussed in detail. It is shown that an entirely different type of heating rate profiles can be obtained if the k_1 and k_2 values are changed by a factor of five.

Examination of the results obtained for the other eight cases indicates that the maximum change in the heating rates is of the order of 8 ^{o}K/day at 62 km for the case when Q_1 and Q_2 are both increased or decreased by 50% (Figure 8b). It is noteworthy that for the same case there was no significant change obtained in the distributions of ozone (Figure 8a).

The other interesting case is shown in Figure (9b) for which maximum changes in ozone concentrations were found (Figure 9a). The heating rates in this particular case do

not increase or decrease uniformly over the normal value, but show an entirely new type of distribution with height. This type of change in the heating of the stratosphere and the mesosphere can have significant dynamical repercussions in the stratosphere. Figures 6b and 7b show that when the changes are only confined to one spectral region (Q_1 or Q_2), the heating rates are more sensitive to Q_2 than Q_1.

Penetration of radiation into the atmosphere

Figures 6c, 7c, 8c, and 9c show the depths of penetration of the near ultraviolet radiation in the earth's atmosphere for each of the nine cases. The solid curve in each figure represents the 'normal' case. The altitudes plotted in the figures correspond to the height where radiation of a particular wavelength is reduced to $\frac{1}{e}$ of its initial value.

The general shape of these curves shows the influence of the strong absorption bands of oxygen and ozone in the near ultraviolet. The radiation in the 1700-2000 Å region is strongly absorbed by oxygen (Schuman-Runge bands) and therefore does not penetrate below the altitude of 50 km. In the spectral region of 2000-2200 Å the absorption due to

both oxygen and ozone is relatively weak and the radiation of these wavelengths penetrates to altitudes as low as 35 km. Above 2300 Å the absorption cross sections of ozone increase rapidly (Hartley bands), reaching a maximum at 2550 Å, and so does the height of penetration of the radiation. At wavelengths longer than 3100 Å the absorption due to ozone is very weak (Huggins band) and the radiation almost reaches the ground.

Examination of the figures 6c, 7c, 8c, and 9c and their comparison with respective ozone distributions, (Figures 6a, 7a, 8a, and 9a) reveals the extreme sensitivity of the penetration depth of the radiation in the 2500 Å region to the ozone distribution in the mesosphere. For the cases where Q_1 and Q_2 have been assumed to change in opposite directions by 50%, the depth of penetration of 2500 Å radiation may vary by as much as 10 km (Figure 9c). For the other extreme case when the change in radiation is uniform over the whole spectral interval, 1700-3000 Å, there is no change in the depth of penetration of the radiation (Figure 8c), mainly because the ozone distribution

has remained unchanged(Figure 8a).

Total Ozone

For each of the nine cases the total integrated ozone amount in a vertical column was also determined. These values have been plotted in Figure 10 (lower curve). On the abscissa are shown the directions in which Q_1 and Q_2 have been changed ty 50% for each of the nine cases. The first case, for example, is when Q_1 and Q_2 are both decreased by 50%. The total ozone value for the case of no change is 0.24 cm-atm. It is noted that for all the other eight cases, the total ozone amount remains approximately within 20% of the normal value.

It is known (see, for instance, Paetzold, 1957) that the observed day to day variations in the total ozone amount at a given station are mainly due to changes in the ozone content of the lower stratosphere, between 10 and 30 km. This is the region of maximum ozone concentration (Fig. 2) and therefore the measurements of total ozone in a vertical column are heavily weighted by the ozone content of this region.

It is also well known (Dütsch, 1961) that the ozone distribution in the atmosphere at altitudes below 30 km is not

in photochemical equilibrium. It is the atmospheric motions which play a dominant role in determining the vertical distribution of ozone in this region.

In Figure 10, upper curve, we have plotted a typical sample of daily total ozone values measured at Edmonton (Canada). It is seen that the magnitude of the day to day variation in the total ozone could be as high as 30% of the mean value.

From the above discussion it is clear that the expected changes in the total ozone due to possible variation in the near ultraviolet radiation intensity, even of the order of $\pm 50\%$, will be difficult to detect.

Discussion

In summary, from the above calculation it has been shown that

1) If the solar radiation in the near ultraviolet from 1700 - 3000 Å increases or decreases uniformly by 50%, the vertical distribution of ozone remains practically unaffected. The heating rates, however, are strongly affected and can increase or decrease by as much as $8^{\circ}K$/day at $\sim$ 60 km altitude for such changes in the solar radiation.

2) The maximum change in the ozone distribution takes place when there is a differential variation of radiation intensity in the near ultraviolet. If the solar flux in the 1700 - 2300 Å region (Q_1) is increased by 50%, at the same time the flux in the 2300 Å - 3000 Å region (Q_2) is decreased by 50%, or vice versa, the concentrations at the altitudes above 40 km are increased or decreased by a factor of two (Fig. 9a). The heating rates in the atmosphere for these changes show an entirely new type of distribution with height (Fig. 9b). For the case when Q_1 is decreased by 50% and Q_2 increased by 50% the heating becomes more extensive at lower altitudes ($\sim$ 40 km) and such a change may have very important meteorological repercussions.

3) Changes in the solar flux which are confined only to either Q_1 or Q_2 regions of near ultraviolet also show changes both in the ozone distributions and in the heating rates, but their magnitude is relatively smaller when compared to the above mentioned two cases.

ACKNOWLEDGEMENT

I am grateful to Professor Julius London of the University of Colorado for many illuminating discussions and helpful suggestions. It is also a pleasure to thank Mr. Conrad Hipkins who expertly programmed and carried out the numerical computations on the IBM 7090.

REFERENCES

Allen, C. W. (1958) Solar Radiation, Quar. Jour. Roy. Met. Soc. 84, p. 307.

Campbell, E. S., and Nudelmann, C., (1960) Reaction kinetics, thermodynamics and transport properties in the ozone oxygen system. AFOSR TN-60-502, New York University.

Detwiler, C. R., D. L. Garrett, J. D. Purcell, and R. Tousey (1961) 'The intensity distribution in the ultraviolet solar spectrum,' Ann. Geophys., 17, 263-292.

Dütsch, H. (1961) 'Current problems of the photochemical theory of atmospheric ozone' in "Chemical reactions in the lower and upper atmosphere." Interscience Publishers, John Wiley & Sons, New York, p. 167.

Hinteregger, H. E. (1962) 'Absorption spectrometric analysis of the upper atmosphere in EUV region,' Jour. Atm. Sciences 19, p. 351-68.

Israël, G. (1963) 'French contribution to the measurement of atmospheric pressure,' Space Research III, North Holland Publishing Company, Ed. W. Priester.

Johnson, F. S., J. D. Purcell, R. Tousey, and N. Wilson (1954) 'The ultraviolet spectrum of the sun,' Rocket Exploration of the upper atmosphere, Pergamon Press Ltd., London, p. 279, Ed. Boyd, R. L. F. and Seaton, M. J.

Kaufman, F. and Kelso, J. R. (1961) 'The homogeneous recombination of atomic oxygen' in "Chemical reactions in the lower and upper atmosphere." Interscience Publishers, John Wiley & Sons, New York, p. 255.

London, J., Ooyama, K., and Prabhakara, C. (1962) 'Mesospheric Dynamics,' Final Report, Contract No. AF 19(604)-5492, New York University.

McAllister, H. C. (1960) A preliminary photometric atlas of the solar ultraviolet spectrum from 1800 to 2965 Å., University of Colorado Printing Services.

Nordberg, W. (1962) 'Temperature Structure in the Mesosphere,' Conference on Circulation and Temperature in the Stratosphere and Mesosphere, Berlin, August 1962.

Nordberg, W. and Stroud, W., Results of IGY rocket-grenade experiments to measure temperatures and winds above the island of Guam, J. G. R. 66, p. 455.

Paetzold, H. K. and E. Regener (1957) Ozon in der Erdatmosphäre. Handbuch der Physik, Band XLVIII, Geophysik II. Springer-Verlag, p. 370.

Stroud, W. G., Nordberg, W., Bandeen, W. R., Batman, F. L. and Titus, P. (1960) Rocket-grenade measurements of temperatures and winds in the mesosphere over Churchill, Canada, J. G. R. 65, 8, p. 2307.

Tanaka, Y., E. C. Y. Inn, and K. Watanabe (1953) Absorption coefficients of ozone in vacuum ultraviolet, Part IV, Ozone. J. Chem. Phy. 21, p. 1651.

Tweles, S. (1961)'Time section and hodograph analysis of Churchill rocket and radiosonde winds and temperature,' Month. Weath. Rev., v. 89, p. 125.

Vigroux, E. (1953) Contributions a l'etude experimentale de l'absorption de l'ozone, Ann. Phys., 8, 709-762.

Watanabe, K. (1958) Ultraviolet absorption processes in the upper atmosphere, Advances in geophysics, vol. 5, Academic Press, Inc. Publishers, New York, p. 154-210.

LEGENDS

Fig. 1. Energy flux outside the earth's atmosphere, after various authors.

Fig. 2. Vertical distribution of ozone in the earth's atmosphere --Curve 1: photochemical equilibrium distribution; Curve 2: observed for the equatorial latitudes.

Fig. 3. Vertical temperature profile based on rocket measurements at Guam.

Fig. 4. Atmospheric density as a function of height, measured at Guam.

Fig. 5. Absorption cross sections in cm^2/molecule in the near ultraviolet for molecular oxygen (curve 1) and ozone (curve 2).

Fig. 6a. Vertical distribution of atmospheric ozone in photochemical equilibrium for three values of ultraviolet flux: 1) 'normal' case, 2) 1700-2300 Å flux increased by 50%, 3) 1700-2300 Å flux decreased by 50%.

Fig. 6b. Variation of heating rates with altitude in ^{o}K/day for the same three cases as Figure 6a.

Fig. 6c. Altitudes at which the radiation of a given wavelength have been depleted by 1/e of its initial value for the three cases in Figure 6a.

Fig. 7a. Vertical distribution of atmospheric ozone in photochemical equilibrium for three values of ultraviolet flux: 1) 'normal' case, 2) solar flux in the 2300-3000 Å region increased by 50%, 3) solar flux in the 2300-3000 Å region decreased by 50%.

Fig. 7b. Variation of heating rates with altitude in ^{o}K/day for the same three cases as Figure 7a.

Fig. 7c. Altitudes at which the radiation of a given wavelength have been depleted by 1/e of its initial value for the three cases in Figure 7a.

Fig. 8a. Vertical distribution of atmospheric ozone in photochemical equilibrium for three values of ultraviolet flux: 1) 'normal' case, 2) solar flux between 1700-3000 Å increased by 50%, 3) solar flux between 1700-3000 Å decreased by 50%.

Fig. 8b. Variation of heating rates with altitude in ^{o}K/day for the same three cases as Figure 8a.

Fig. 8c. Altitudes at which the radiation of a given wavelength have been depleted by 1/e of its initial value for the three cases in Figure 8a.

Fig. 9a. Vertical distribution of atmospheric ozone in photochemical equilibrium for three values of ultraviolet flux: 1) 'normal' case, 2) solar flux in 1700-2300 Å interval increased by 50% while 2300-3000 Å interval was decreased by 50%, 3) solar flux in 1700-2300 Å interval decreased by 50% while 2300-3000 Å interval increased by 50%.

Fig. 9b. Variation of heating rates with altitude in ^{o}K/day for the same three cases as Figure 9a.

Fig. 9c. Altitudes at which the radiation of a given wavelength have been depleted by 1/e of its initial value for the three cases in Figure 9a.

Fig. 10. The lower curve shows the variation in the total ozone in cm-atm for nine different cases of changes in solar flux in the near ultraviolet. The upper curve shows typical day to day changes in total ozone amount recorded at Edmonton, Canada, during the summer of 1962.

APPENDIX I

PROPOSAL FOR MEASURING TIME VARIATIONS IN THE SOLAR ULTRAVIOLET RADIATION (1800 Å - 3000 Å) BY AN EARTH SATELLITE

S. I. Rasool

I. Proposed Experiment

An experiment is proposed in which a small apparatus will be flown in a satellite to obtain a continuous measure of the total intensity in the near ultraviolet region of the solar spectrum over a period of a few months.

The apparatus consists of filters and photoelectric detectors. The experiment is concerned with the spectral regions of 1800 - 2200 Å and 2200 - 3000 Å, being the regions which control the thermal balance of the stratosphere. The experiment will permit us to determine the changes in the intensity of the near ultraviolet during times of solar activity. It will provide our first direct information on the relation between anomalous changes in solar activity and conditions in the lower atmosphere.

II. Background

The complete ultraviolet spectrum of the sun was photographed for the first time in 1946, with the help of V-2 rockets. Since then, numerous rocket experiments have been carried out and a large number of spectrograms obtained; but, surprisingly, nearly all of them concern the extreme ultraviolet (Friedman 1960). The very few available spectra of the near ultraviolet are so fragmentary and widely spaced in time that no information can be obtained regarding their variation in intensity with the changes in solar activity.

III. Influence of the Near UV Radiation on the Properties of the Stratosphere

The 1800 - 3000 Å incoming solar radiation is responsible for the formation of the ozone layer in the upper stratosphere, and thus for the temperature maximum of the stratopause (about 50 km). The ozone equilibrium is governed by the following photochemical reactions:

$$O_2 + h\nu \ (1800 - 2300 \text{ Å}) \rightarrow O + O$$

$$O + O_2 + M \rightarrow O_3 + M$$

$$O_3 + h\nu \ (2200 - 3000 \text{ Å}) \rightarrow O + O_2$$

Any sudden or long-period change in intensity in this ultraviolet region will affect the equilibrium of the ozone layer, which may in turn affect the temperature distribution of the stratosphere to produce a wide-scale meteorological repercussion.

One of the most intriguing problems in atmospheric physics at present is the possible response of the earth's lower atmosphere to solar perturbations. Recently many workers have found observational evidence that anomalous changes in solar activity produce an appreciable effect on certain meteorological phenomena in the troposphere and lower stratosphere. Shernaq (1960) has shown that the "explosive" stratospheric warmings over Europe in January and July of 1958 were preceded by intense solar activity. Asakura and Katayama (1958) have associated sudden reversals in 500 mb atmospheric circulation patterns with the occurrence of solar flares. Rasool and Vassy (1960) report increased ozone amounts over Europe during the solar cycle maximum of 1957-1958, while individual solar flares also appear to be followed by sudden but small increases in the total ozone amounts.

These and other recent results (Rasool 1961) suggest that a coupling between the upper and lower atmosphere does exist. However, a feasible mechanism is yet to be found which could explain the amplification of the relatively small energy changes at the top of the atmosphere into large-scale meteorological distrubances in the lower atmosphere.

IV. Importance of Ozone

One of the mechanisms by which a link between the solar activity and the lower atmospheric phenomena can be established is by the influence of solar ultraviolet flux on the ozone content of the atmosphere. According to the above-mentioned equations as summarized by Deutsch (1960).

1) A uniform change over the entire UV would allow more absorption by ozone, with an increase in temperature, and a decrease in equilibrium amount;

2) An increase in the radiation of 1800-2200 Å only would give more ozone, but, because of more ozone absorption, the equilibrium would return to initial values;

3) A decrease in the 2200-3000 Å radiation would also increase the amount of ozone, but, because of the decrease in radiation, would not give a higher temperature.

Any or all of these mechanisms could be operating in nature, but no definite conclusions can be derived unless the solar near-ultraviolet flux in both the spectral bands of 1800 - 22000 Å and 22000 - 3000 Å is actually measured above the ozone layer, over a continuous specified length of time. If the proposed measurement of the near UV can be added to the payload of the orbiting solar observatory, we will have our first opportunity to study these suggested mechanisms for energy amplification between the upper and lower atmosphere.

If the proposal is accepted, a design of the apparatus can be submitted.

Asakura T. & Katayama A. (1958) Pap. Meteo. Geoph. 9.15.

Dæutsch, H. (1960) Lake Arrowhead Seminar on Solar-Terrestrial Relationships.

Friedman, H. (1960) Physics of the Upper Atmosphere, Ed. J. Ratcliffe, Ac. Press, New York.

Rasool, S. I. & Vassy A. (1960) C. R. 250 p. 3865.

Rasool, S. I. (1961) Geoph. Pura & Apl., Vol. 48, pp. 93-101.

Sherhag, R. (1960) J. Meteo., Dec., 575-582.

May 11, 1961

APPENDIX II

Fig. (A-1) shows the five different vertical distributions of atmospheric ozone in photochemical equilibrium obtained using five different pairs of values for K_1 and K_2. Curve 1 shows the distribution of ozone for K_1 and K_2 values employed in the original calculations. Curves 2, 3, 4 and 5 show effects on calculated ozone distribution when K_1 and K_2 values are increased or decreased by a factor of five.

Fig. (A-2) shows the vertical distribution of heating rates for the same five cases.

LEGENDS

Fig. A1. Vertical distribution of ozone in photochemical equilibrium for five different combinations of the rate coefficient values, k_1 and k_2.

Fig. A2. Variation of heating rates with altitude computed for the five cases shown in Figure A1.

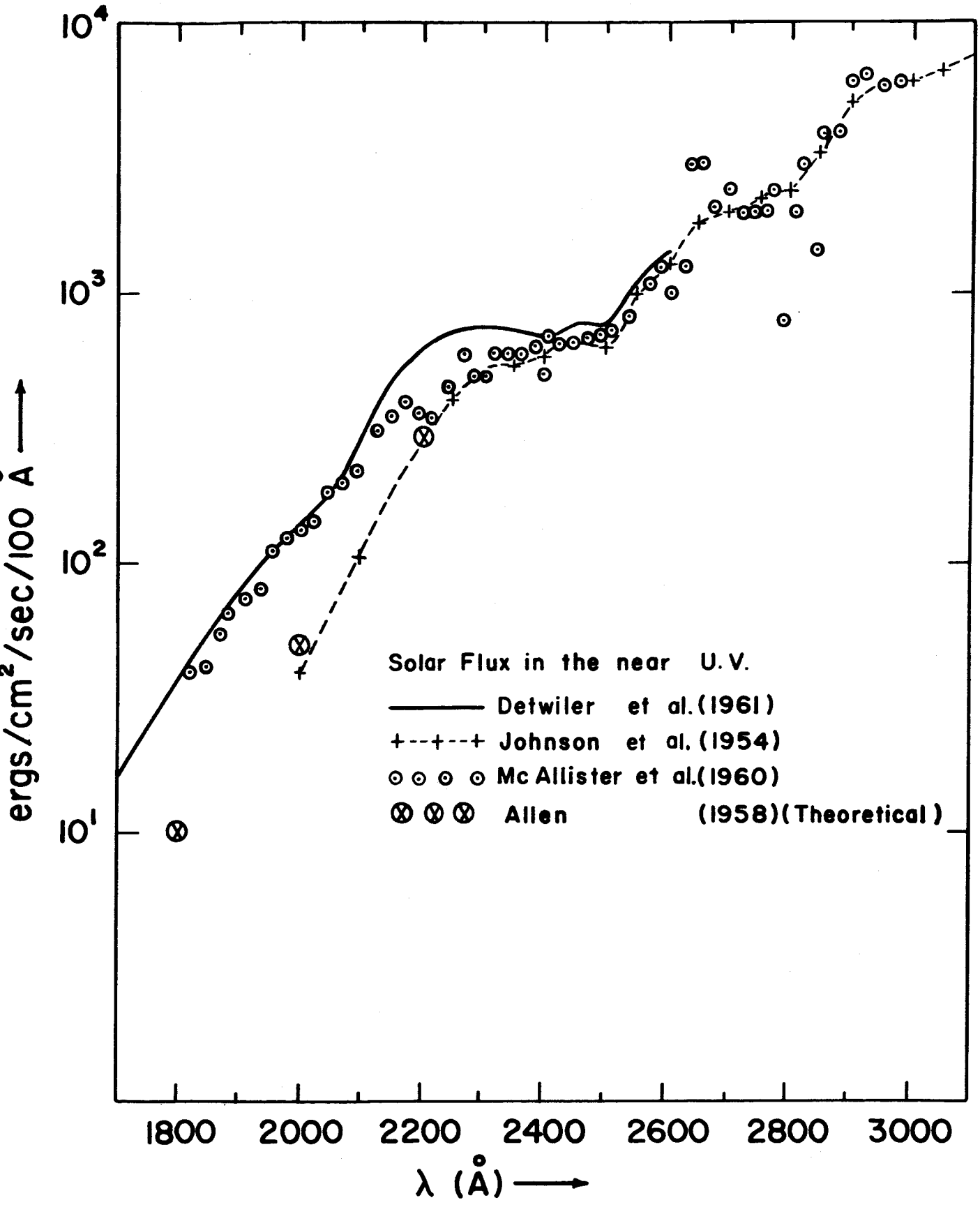
10^4
10^3
10^2
10^1
ergs/cm²/sec/100 Å
1800
2000
2200
2400
2600
2800
3000
λ (Å)
Solar Flux in the near U.V.
Detwiler et al.(1961)
Johnson et al. (1954)
Mc Allister et al.(1960)
Allen (1958)(Theoretical)

Fig. 1

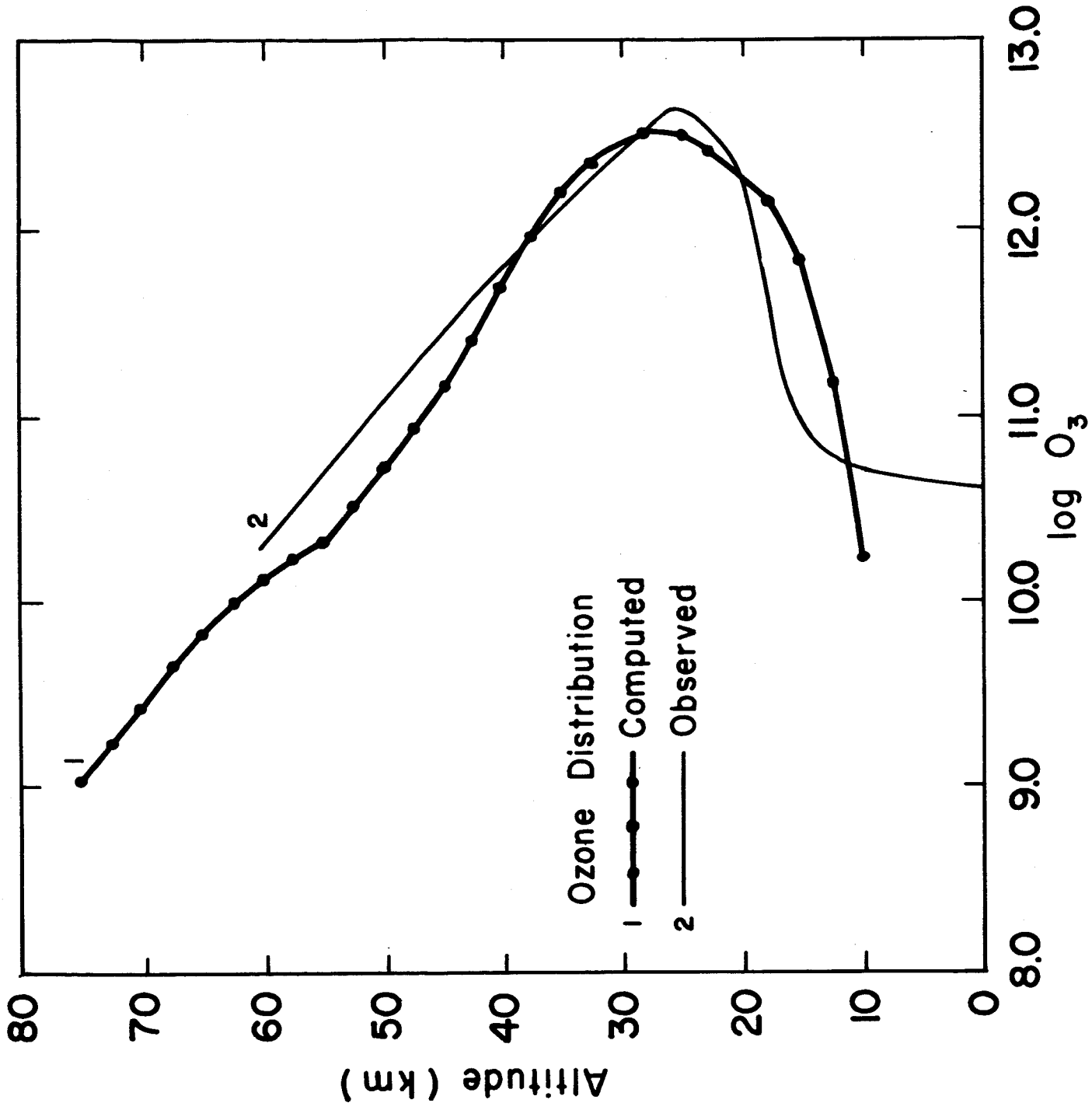
Ozone Distribution
1 Computed
2 Observed
Altitude (km)
log O_3
80
70
60
50
40
30
20
10
0
8.0
9.0
10.0
11.0
12.0
13.0
1
2

Fig. 2

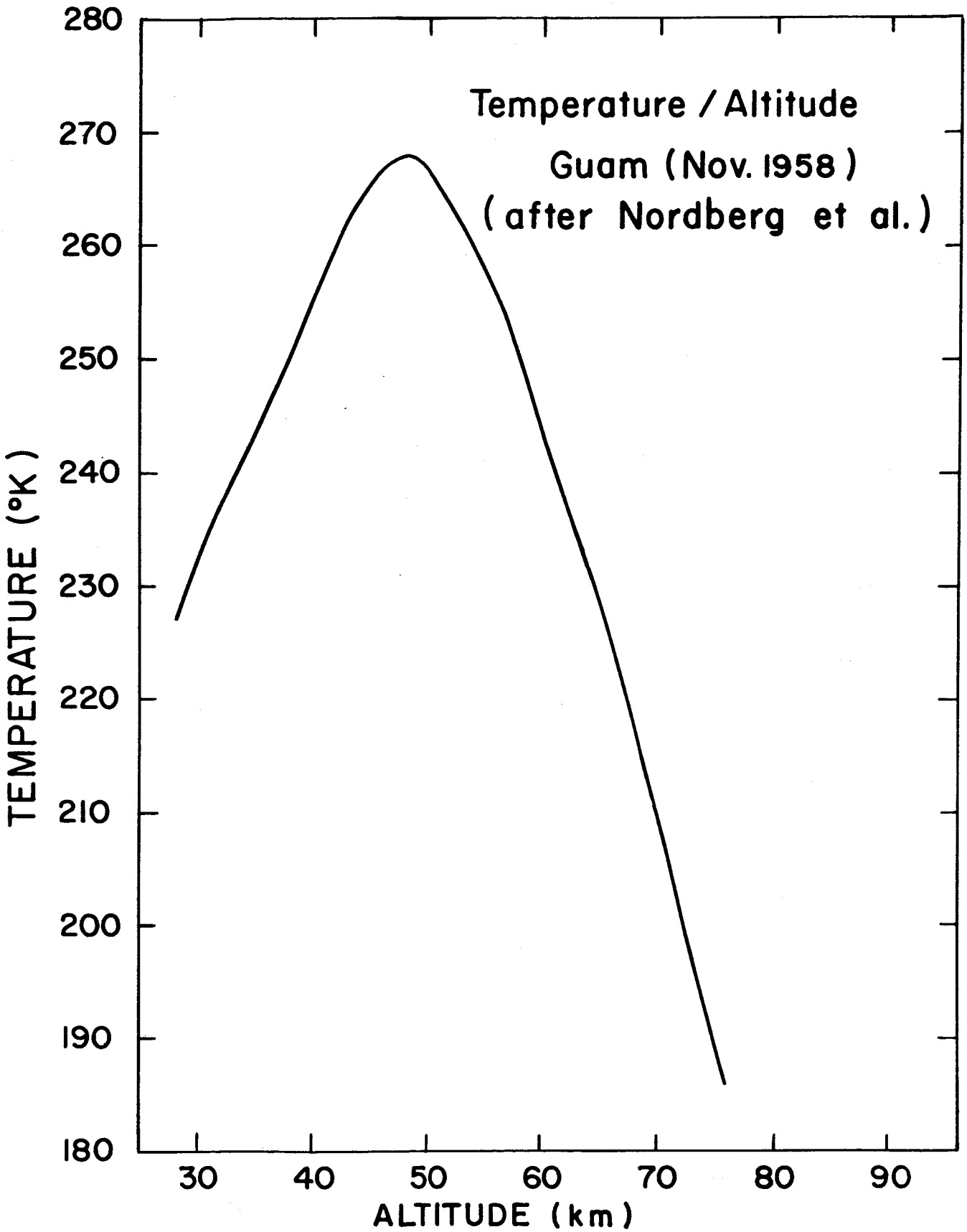
Temperature / Altitude
Guam (Nov. 1958)
(after Nordberg et al.)
TEMPERATURE (°K)
280
270
260
250
240
230
220
210
200
190
180
30
40
50
60
70
80
90
ALTITUDE (km)

Fig. 3

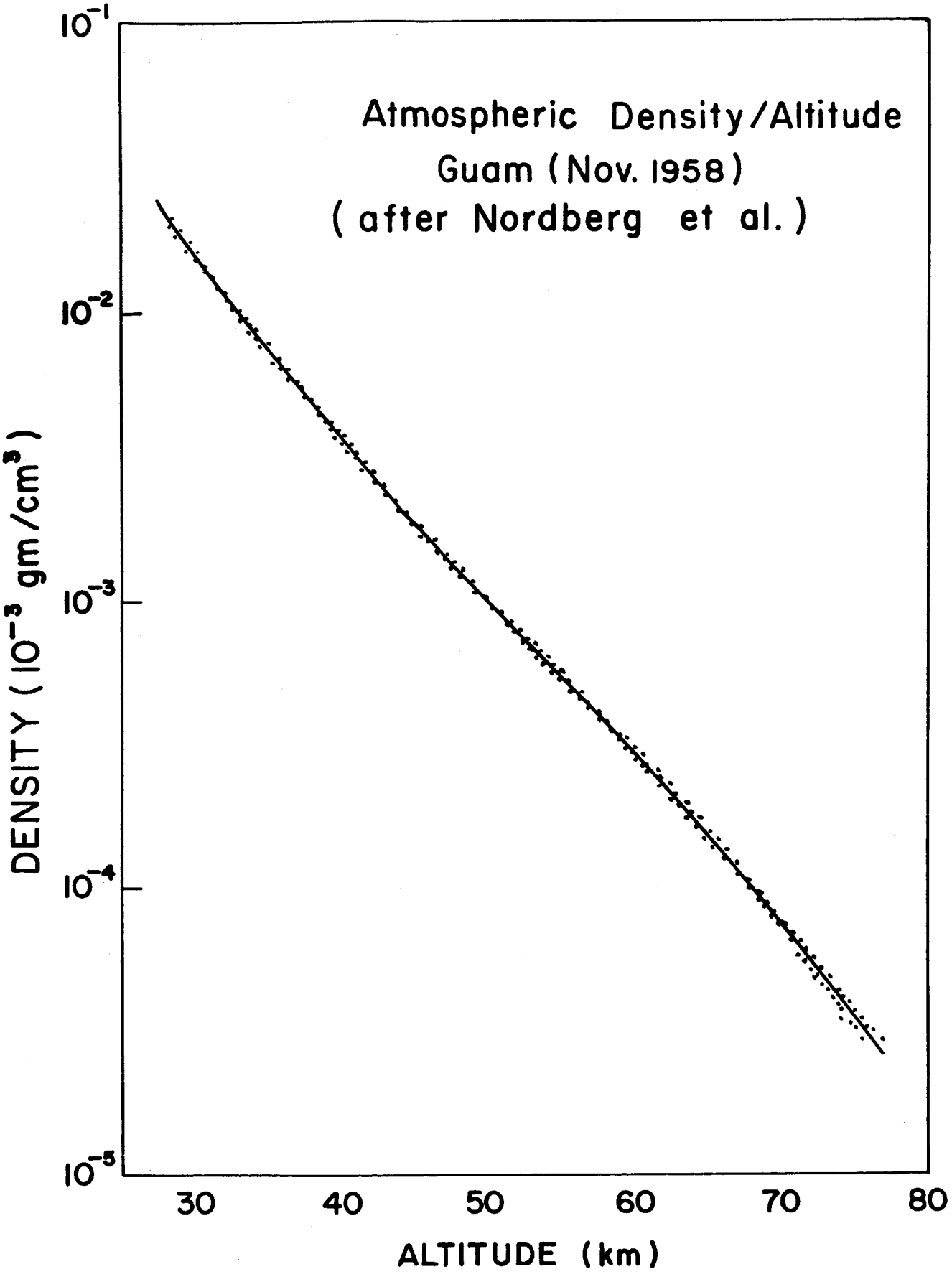
Atmospheric Density/Altitude
Guam (Nov. 1958)
(after Nordberg et al.)
DENSITY (10^{-3} gm/cm^3)
10^{-1}
10^{-2}
10^{-3}
10^{-4}
10^{-5}
30
40
50
60
70
80
ALTITUDE (km)

Fig. 4

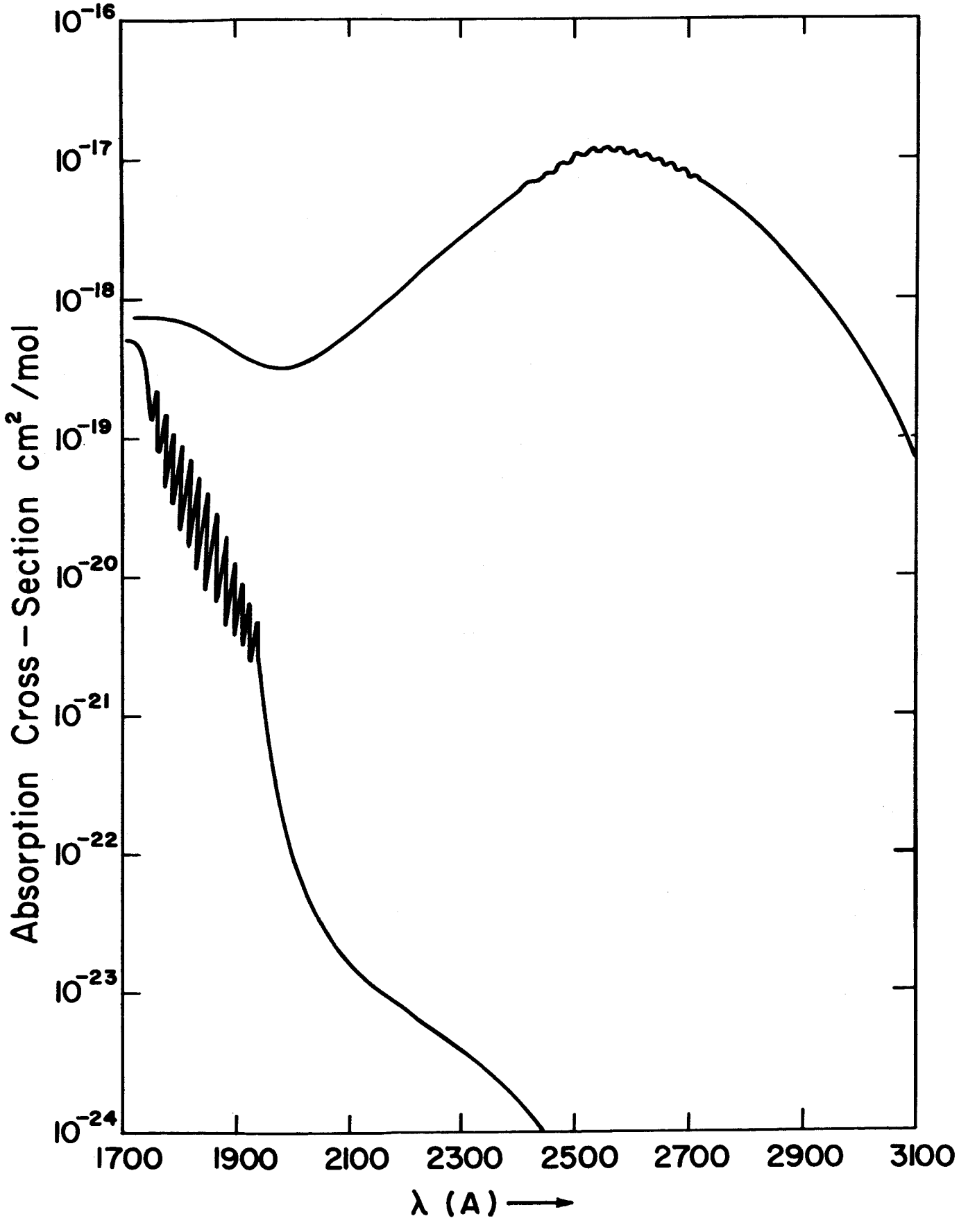
10^{-16}
10^{-17}
10^{-18}
10^{-19}
10^{-20}
10^{-21}
10^{-22}
10^{-23}
10^{-24}
Absorption Cross-Section cm^2/mol
1700
1900
2100
2300
2500
2700
2900
3100
λ (A) ⟶

Fig. 5

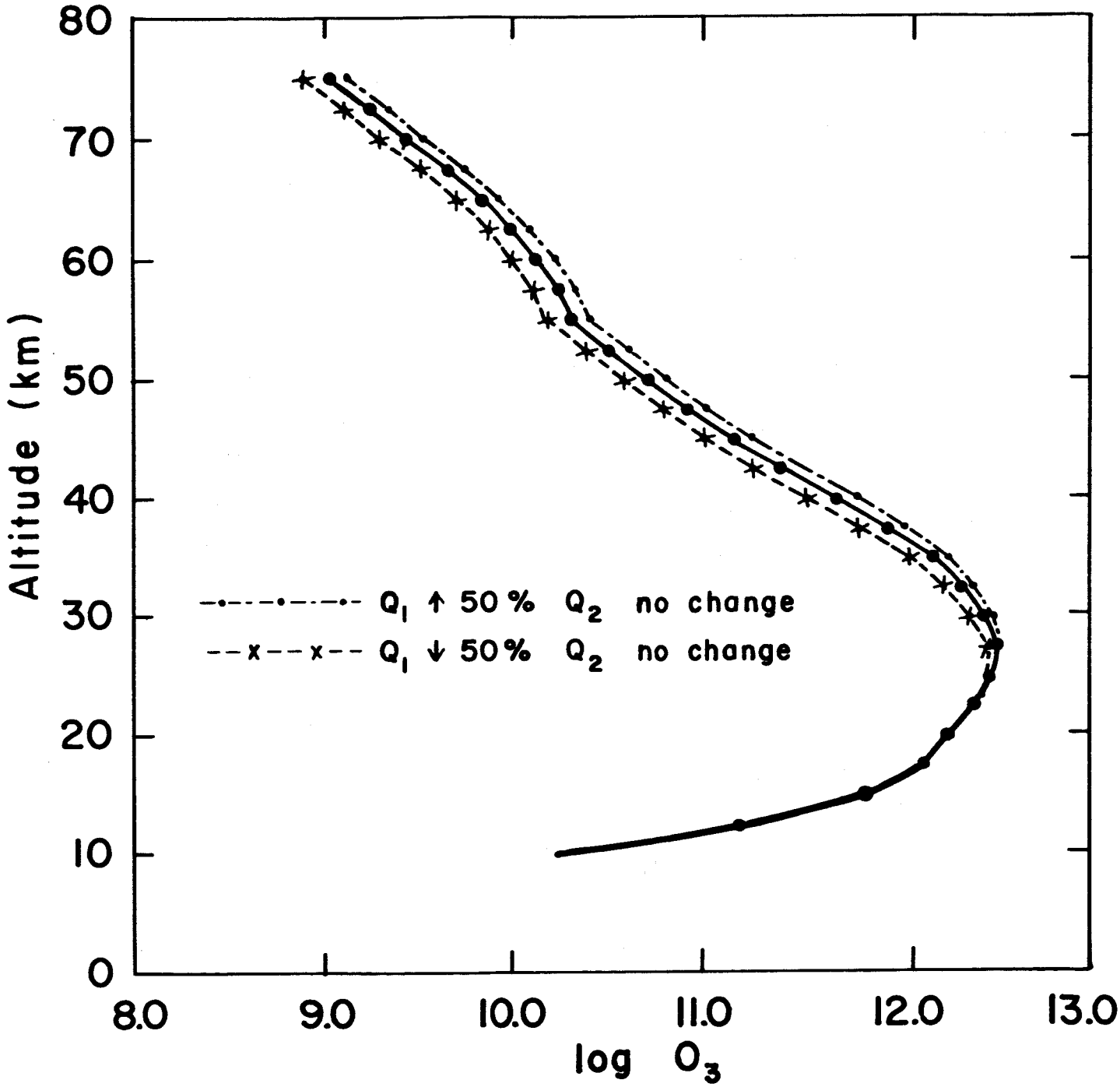
80
70
60
50
40
30
20
10
0
Altitude (km)
8.0
9.0
10.0
11.0
12.0
13.0
log O_3
Q_1 ↑ 50 % Q_2 no change
Q_1 ↓ 50 % Q_2 no change

Fig. 6a

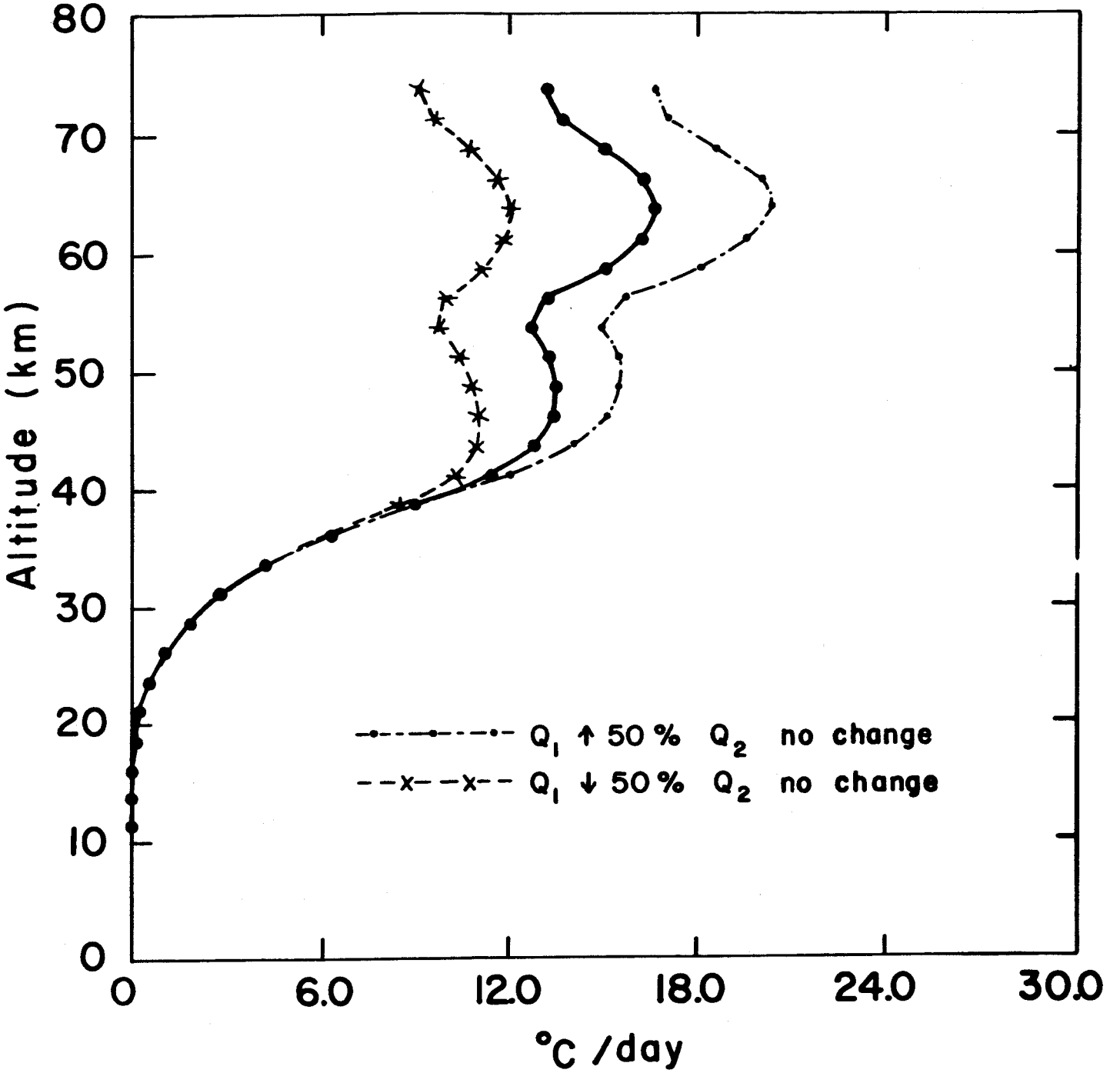
80
70
60
50
40
30
20
10
0
Altitude (km)
0
6.0
12.0
18.0
24.0
30.0
°C /day
Q1 ↑ 50 % Q2 no change
Q1 ↓ 50 % Q2 no change

Fig. 6b

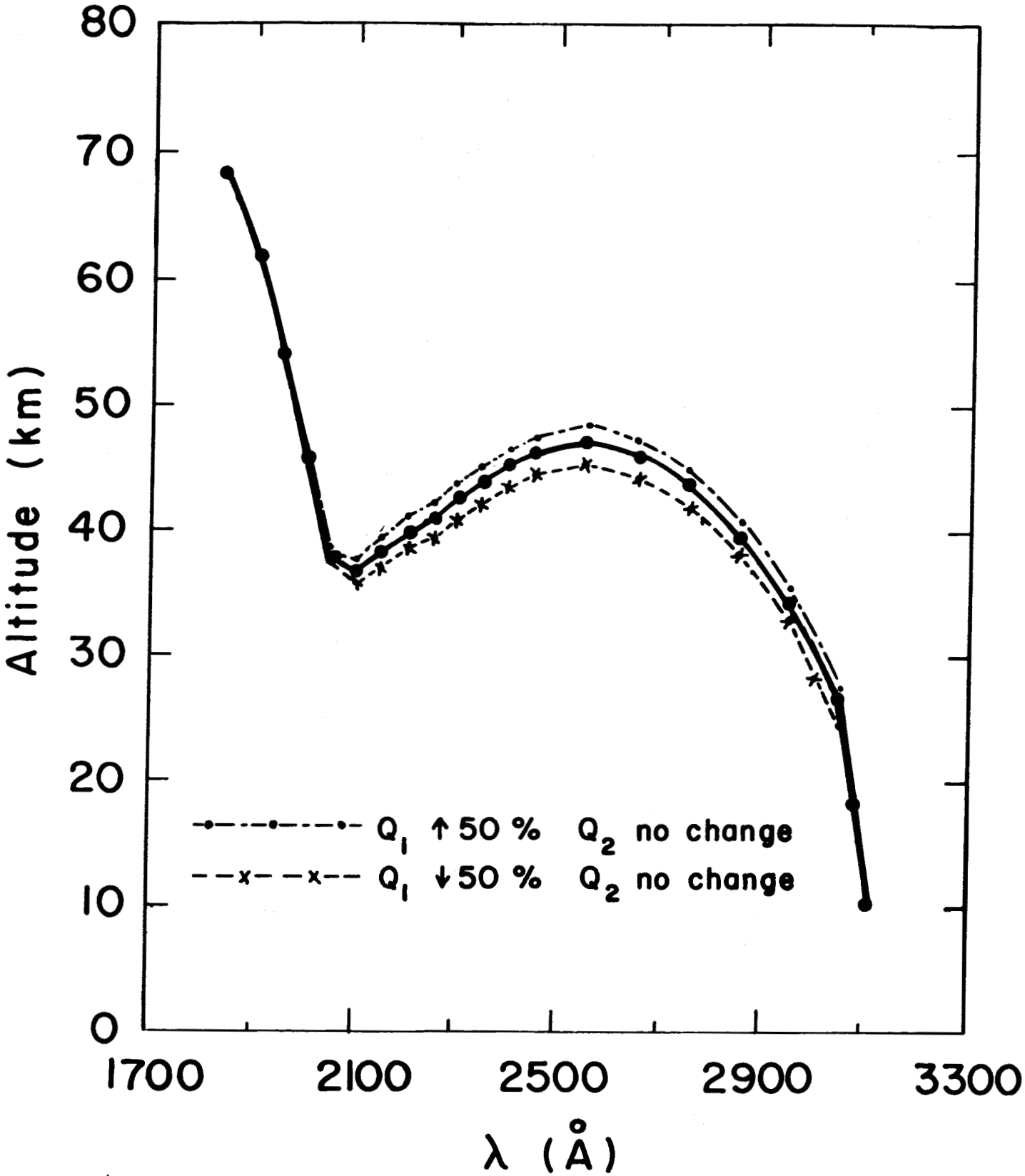
80
70
60
50
40
30
20
10
0
Altitude (km)
1700
2100
2500
2900
3300
λ (Å)
Q1 ↑50 % Q2 no change
Q1 ↓50 % Q2 no change

Fig. 6c

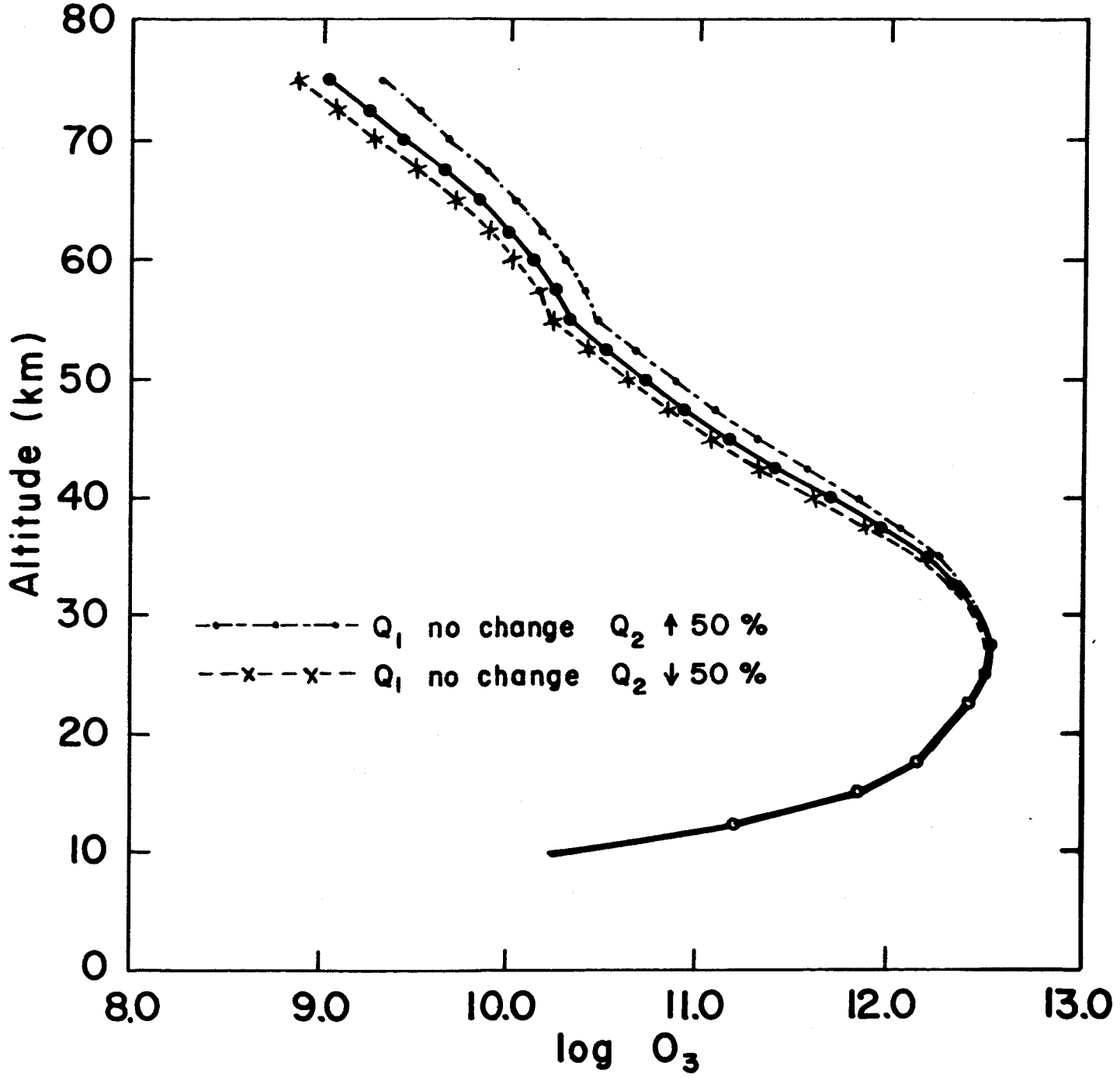
80
70
60
50
40
30
20
10
0
Altitude (km)
8.0
9.0
10.0
11.0
12.0
13.0
log O_3
Q_1 no change Q_2 ↑ 50 %
Q_1 no change Q_2 ↓ 50 %

Fig. 7a

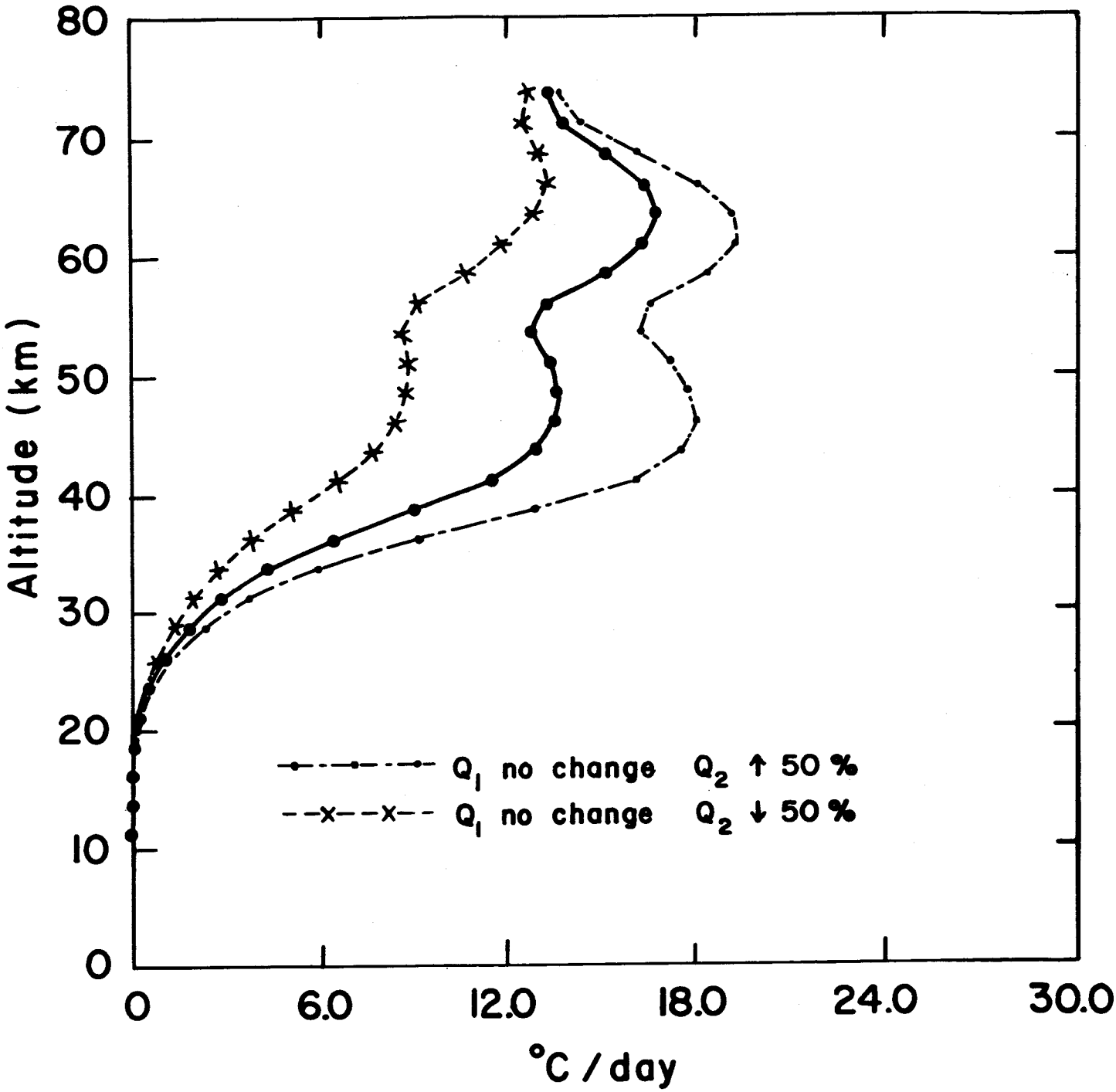
80
70
60
50
40
30
20
10
0
Altitude (km)
0
6.0
12.0
18.0
24.0
30.0
°C / day
Q1 no change Q2 ↑ 50 %
Q1 no change Q2 ↓ 50 %

Fig. 7b

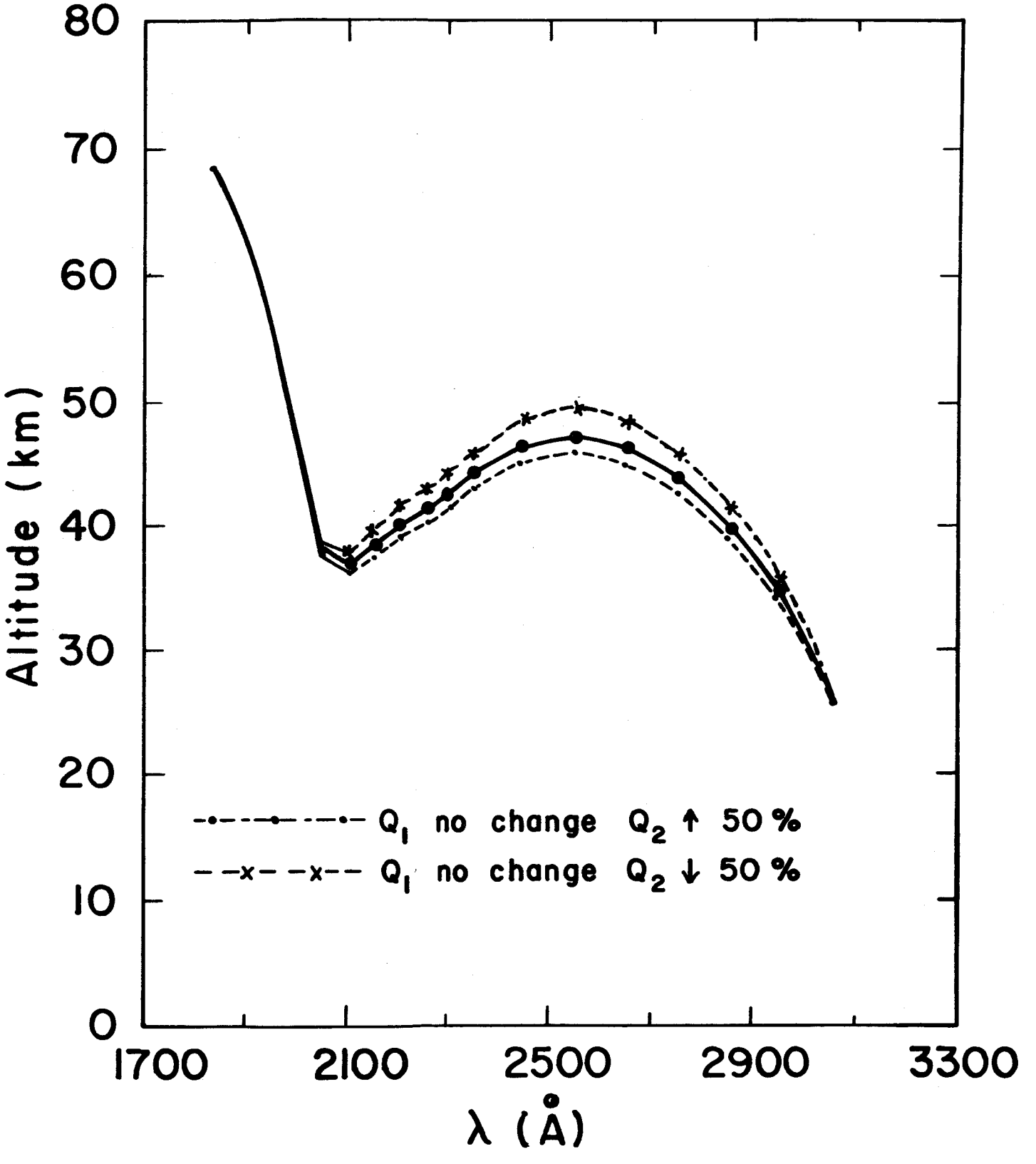
80
70
60
50
40
30
20
10
0
Altitude (km)
1700
2100
2500
2900
3300
λ (Å)
Q1 no change Q2 ↑ 50 %
Q1 no change Q2 ↓ 50 %

Fig. 7c

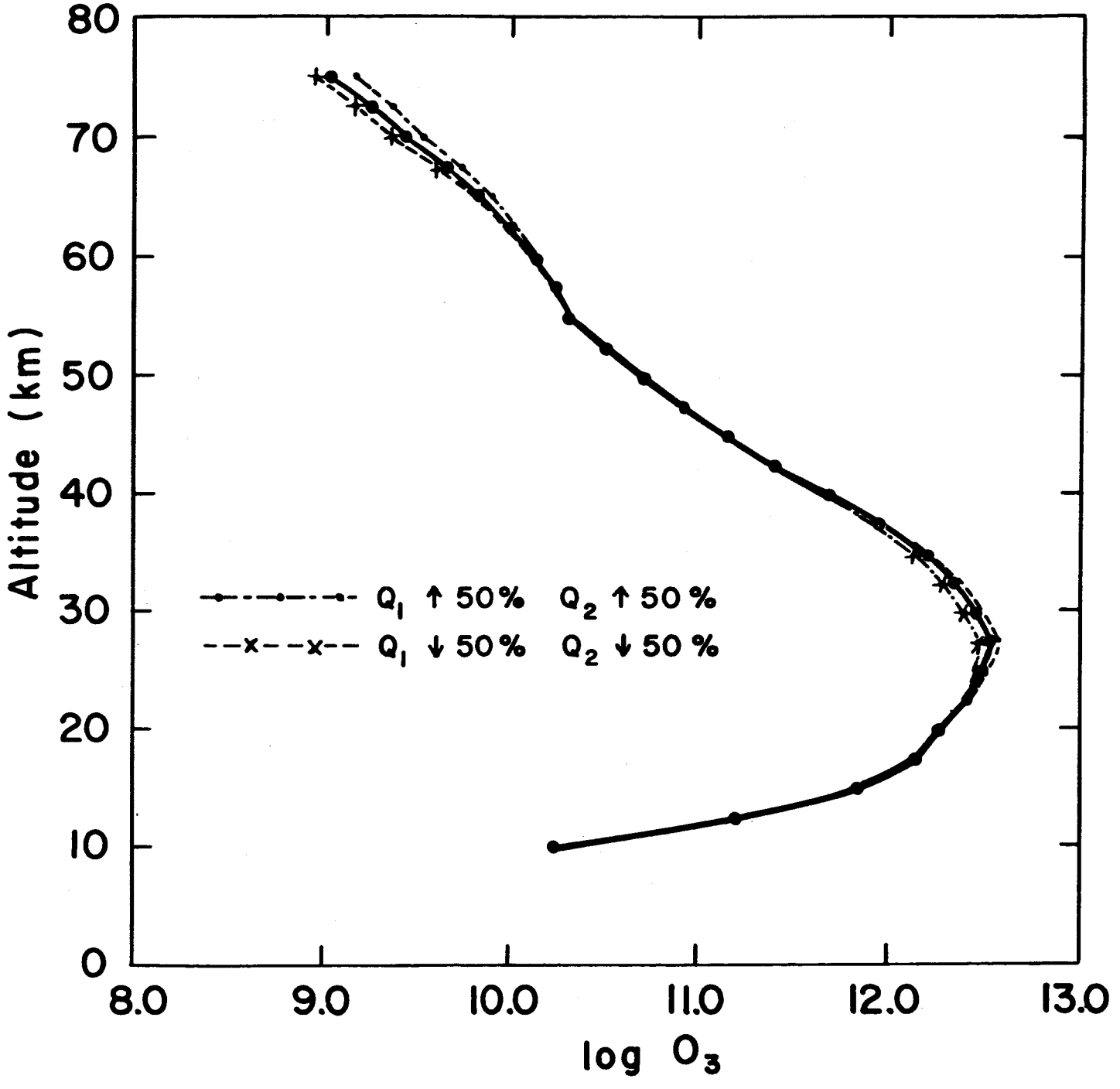
80
70
60
50
40
30
20
10
0
Altitude (km)
8.0
9.0
10.0
11.0
12.0
13.0
log O_3
Q_1 ↑ 50% Q_2 ↑ 50%
Q_1 ↓ 50% Q_2 ↓ 50%

Fig. 8a

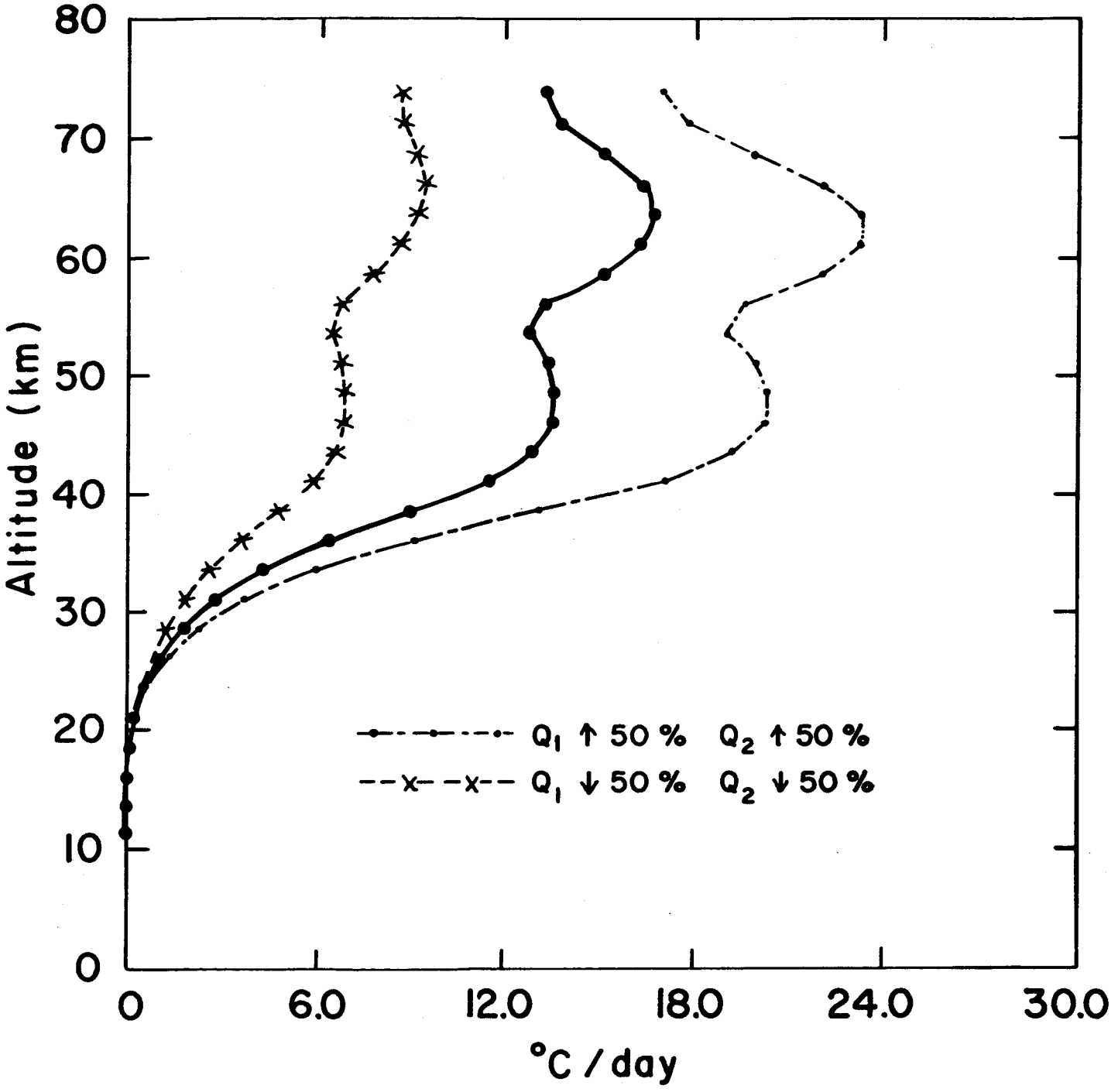
80
70
60
50
40
30
20
10
0
Altitude (km)
0
6.0
12.0
18.0
24.0
30.0
°C / day
Q1 ↑ 50 % Q2 ↑ 50 %
Q1 ↓ 50 % Q2 ↓ 50 %

Fig. 8b

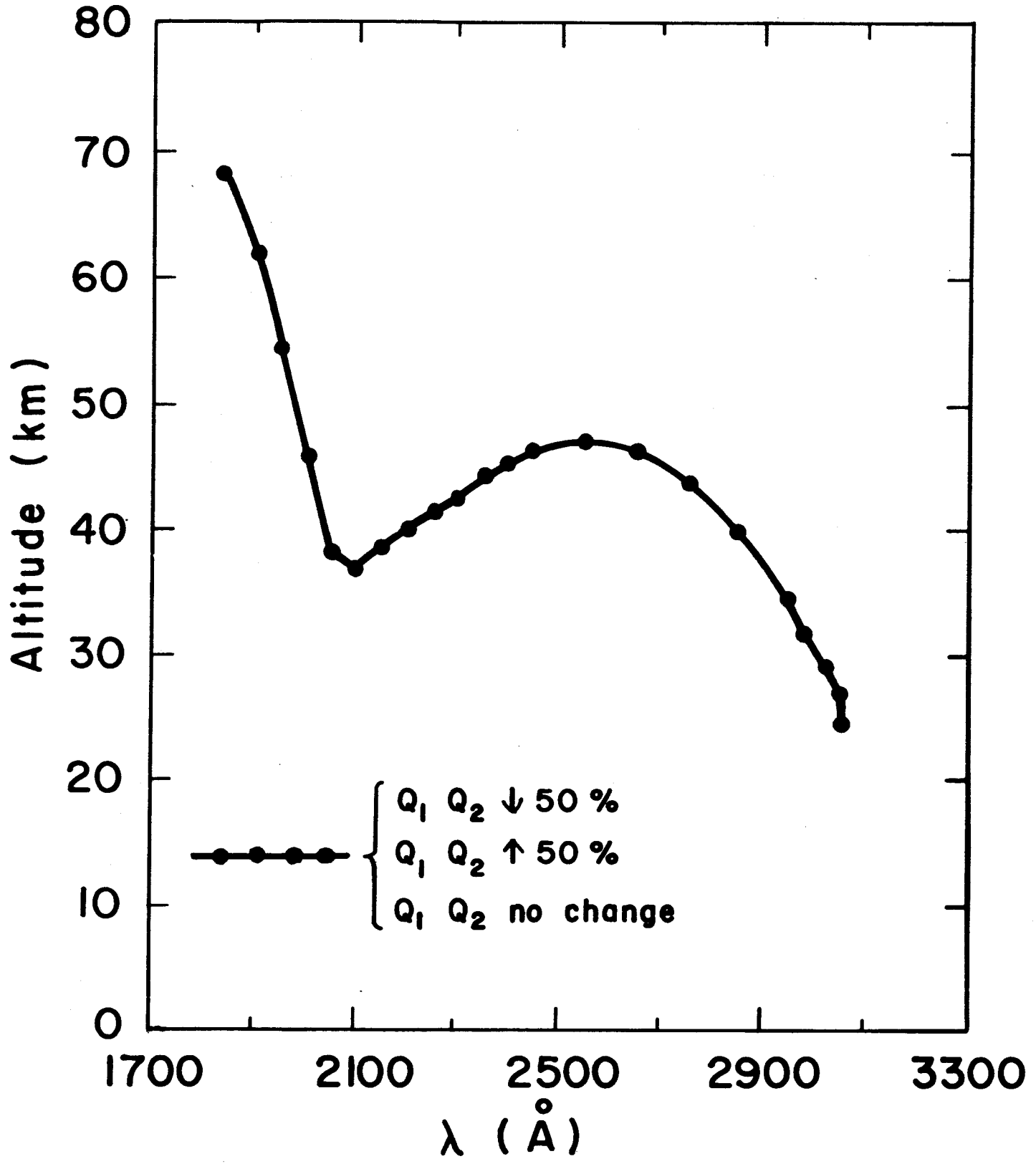
80
70
60
50
40
30
20
10
0
Altitude (km)
1700
2100
2500
2900
3300
λ (Å)
Q_1 Q_2 ↓ 50 %
Q_1 Q_2 ↑ 50 %
Q_1 Q_2 no change

Fig. 8c

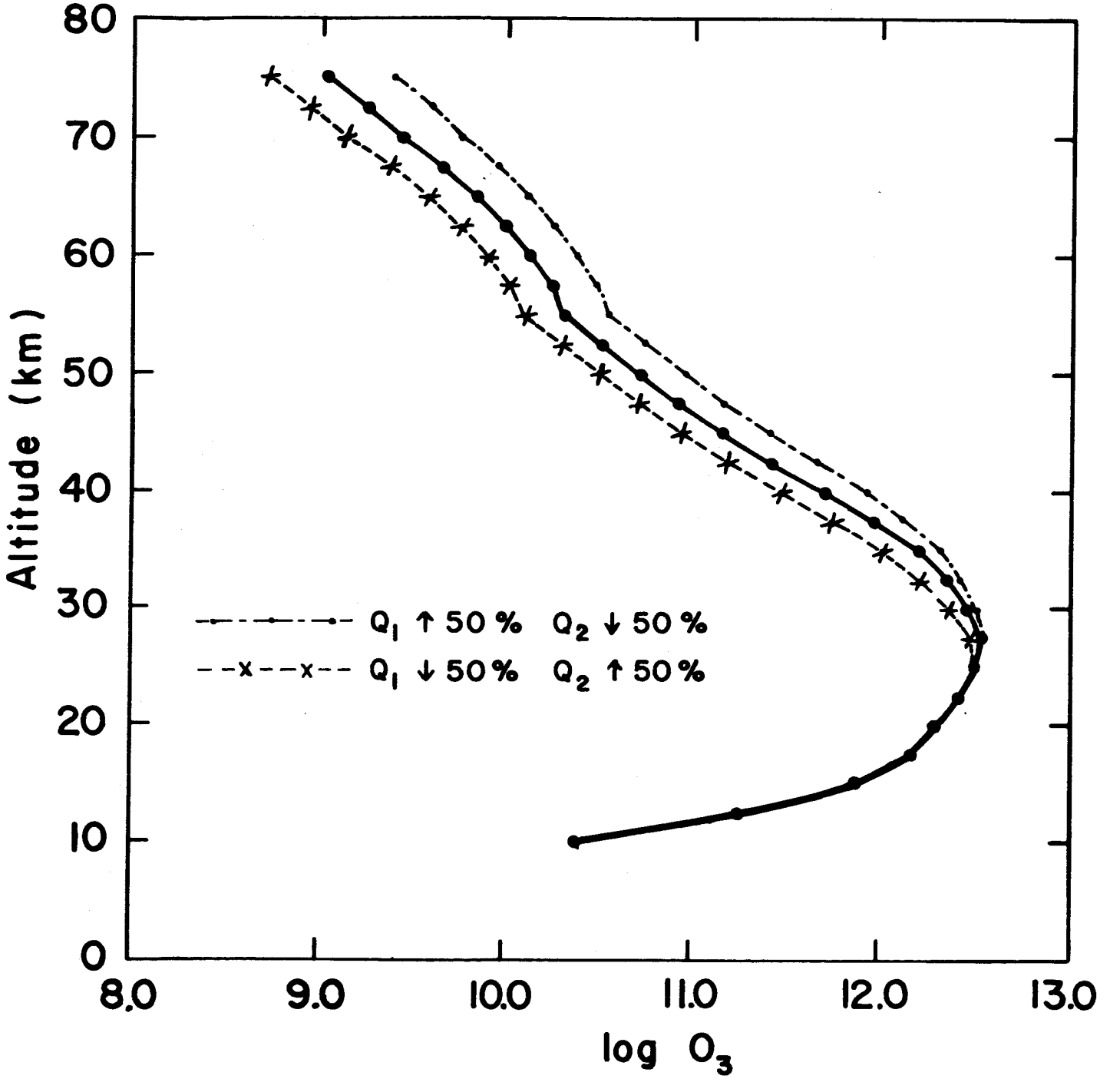
80
70
60
50
40
30
20
10
0
Altitude (km)
8.0
9.0
10.0
11.0
12.0
13.0
log O_3
Q_1 ↑ 50 % Q_2 ↓ 50 %
Q_1 ↓ 50 % Q_2 ↑ 50 %

Fig. 9a

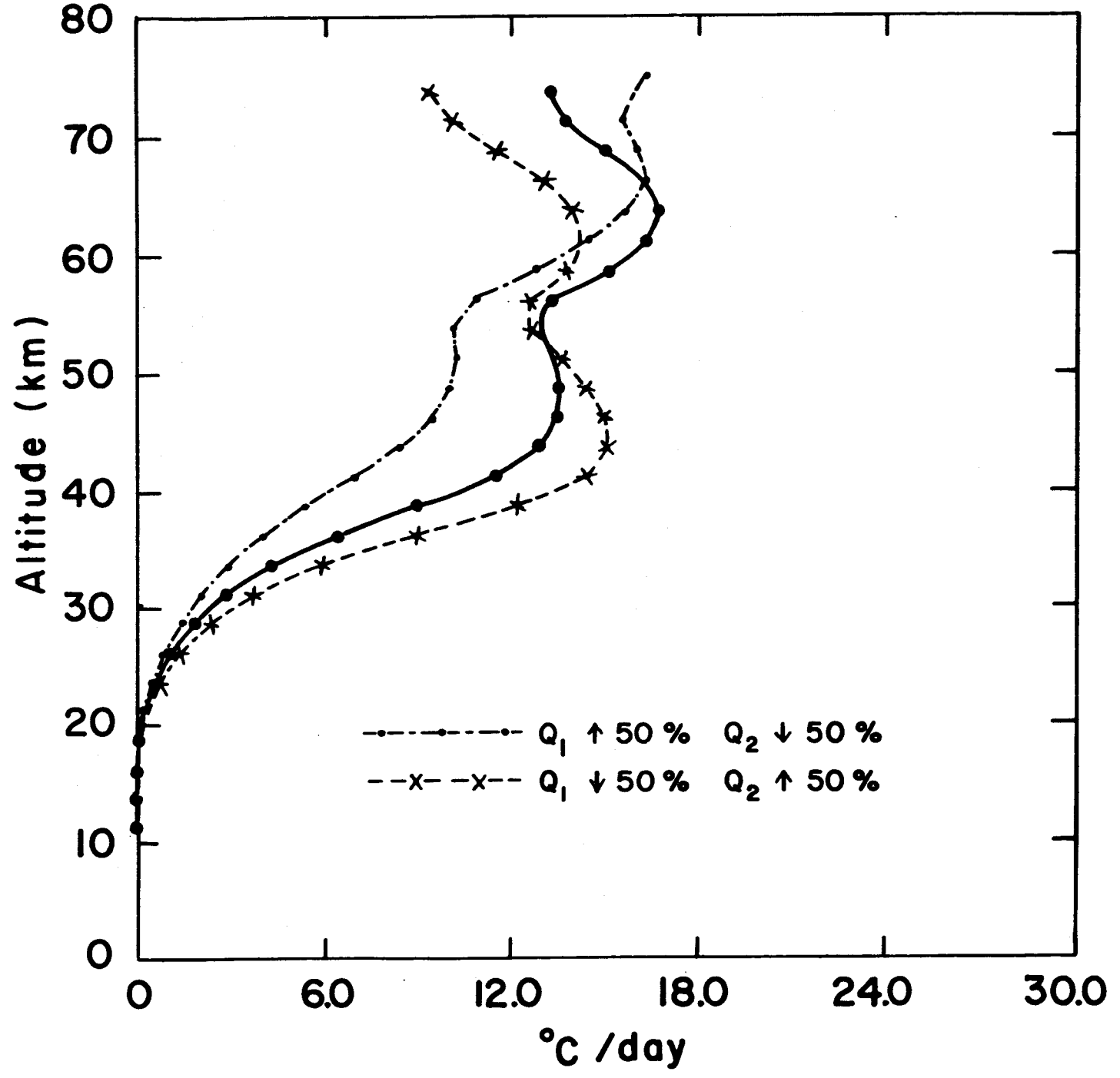
80
70
60
50
40
30
20
10
0
Altitude (km)
0
6.0
12.0
18.0
24.0
30.0
°C /day
Q1 ↑ 50 % Q2 ↓ 50 %
Q1 ↓ 50 % Q2 ↑ 50 %

Fig. 9b

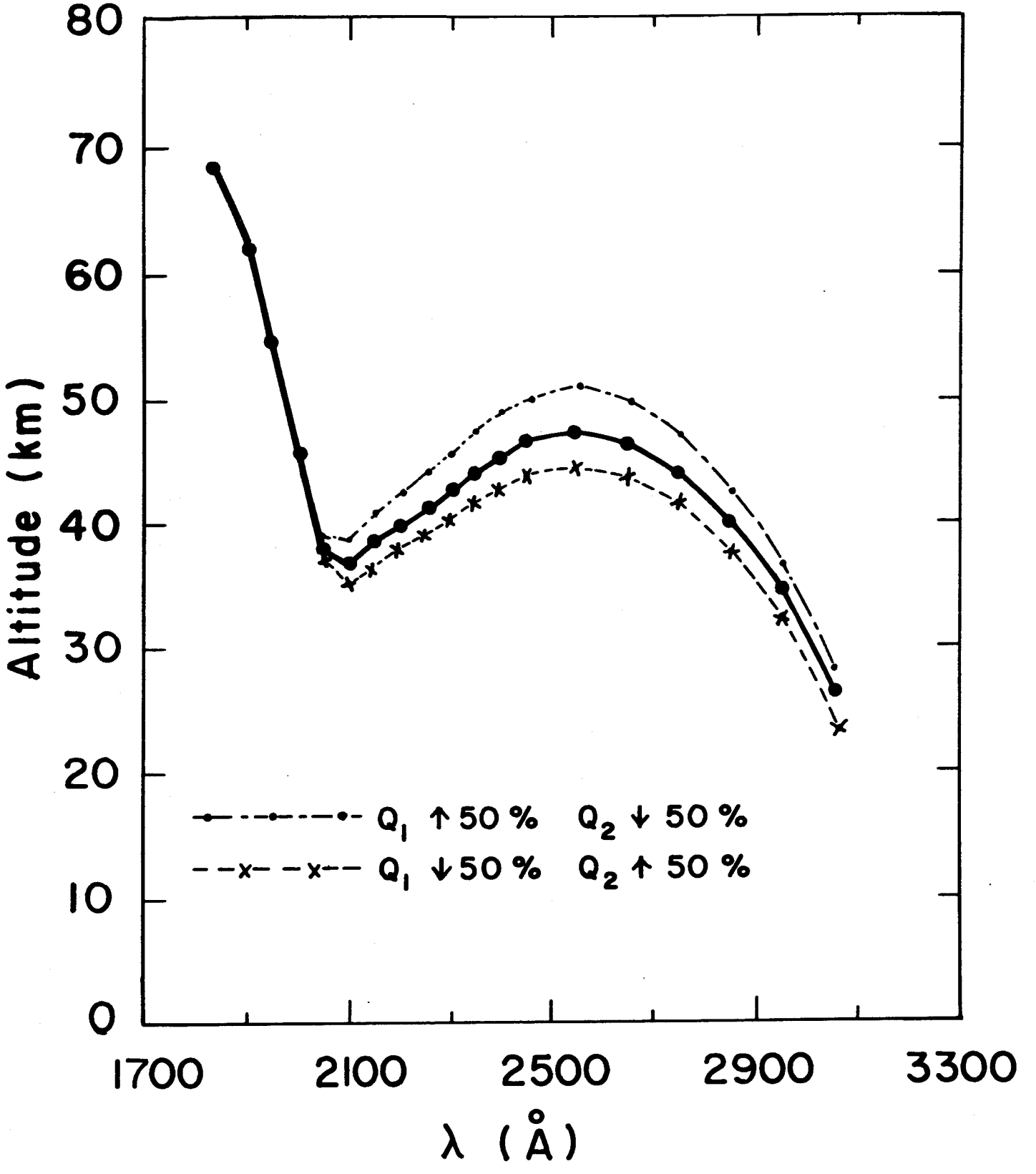
80
70
60
50
40
30
20
10
0
Altitude (km)
1700
2100
2500
2900
3300
λ (Å)
Q1 ↑ 50 % Q2 ↓ 50 %
Q1 ↓ 50 % Q2 ↑ 50 %

Fig. 9c

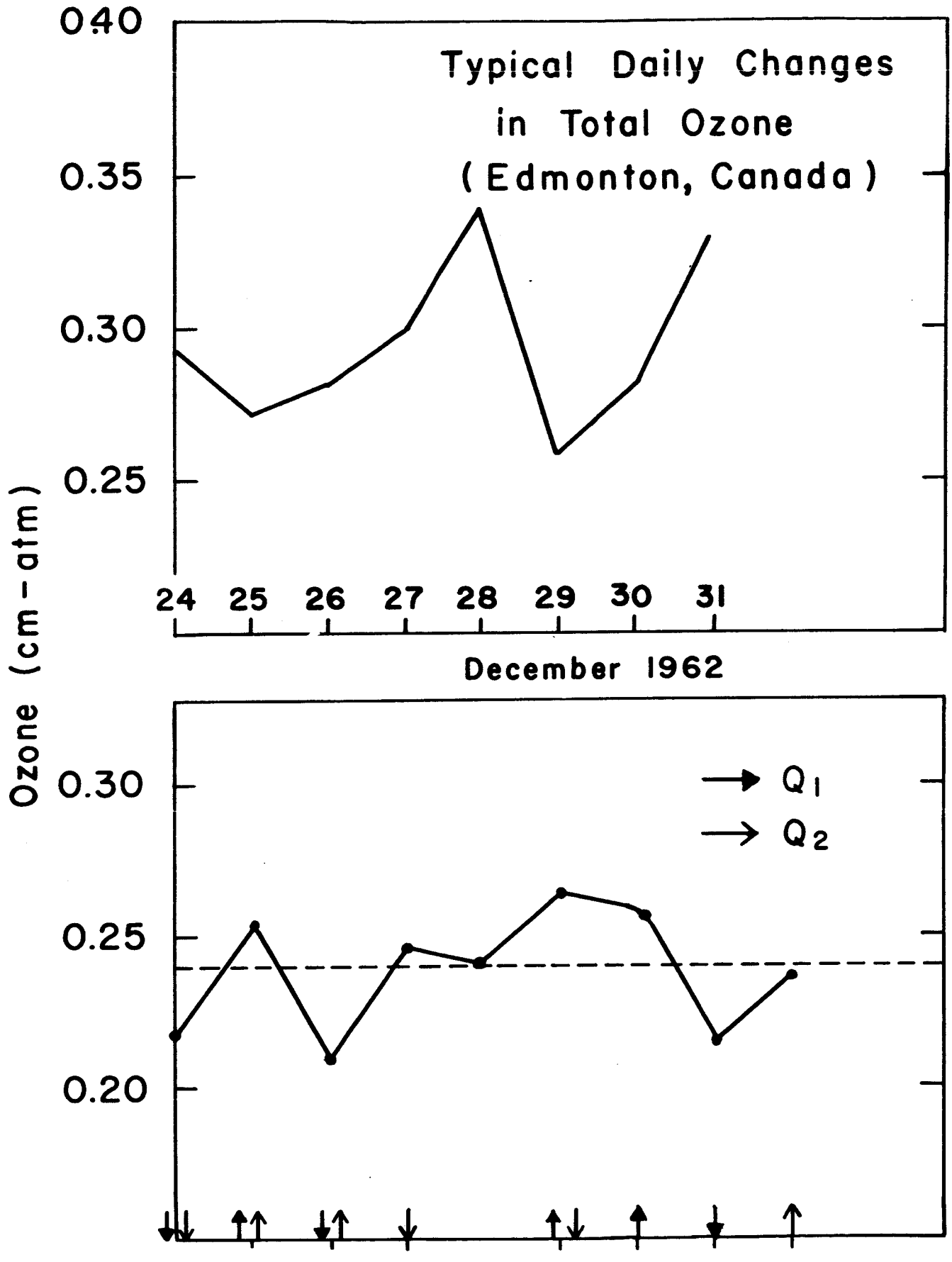
Typical Daily Changes
in Total Ozone
(Edmonton, Canada)
0.40
0.35
0.30
0.25
Ozone (cm-atm)
24 25 26 27 28 29 30 31
December 1962
0.30
0.25
0.20
Q1
Q2

Fig. 10

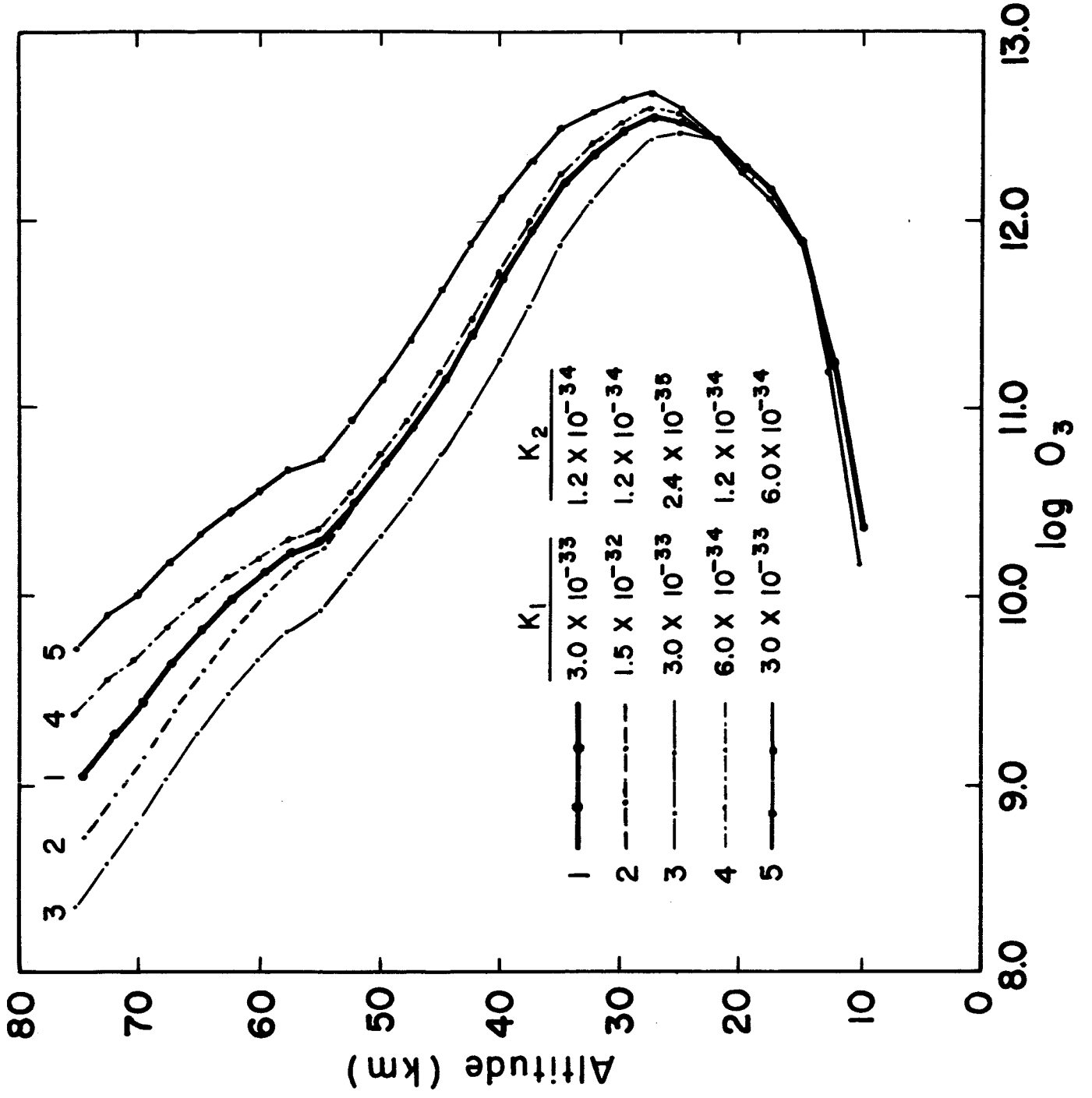
Altitude (km)
log O_3
K_1
K_2
1 3.0 X 10^{-33} 1.2 X 10^{-34}
2 1.5 X 10^{-32} 1.2 X 10^{-34}
3 3.0 X 10^{-33} 2.4 X 10^{-35}
4 6.0 X 10^{-34} 1.2 X 10^{-34}
5 3.0 X 10^{-33} 6.0 X 10^{-34}

Fig. A-1

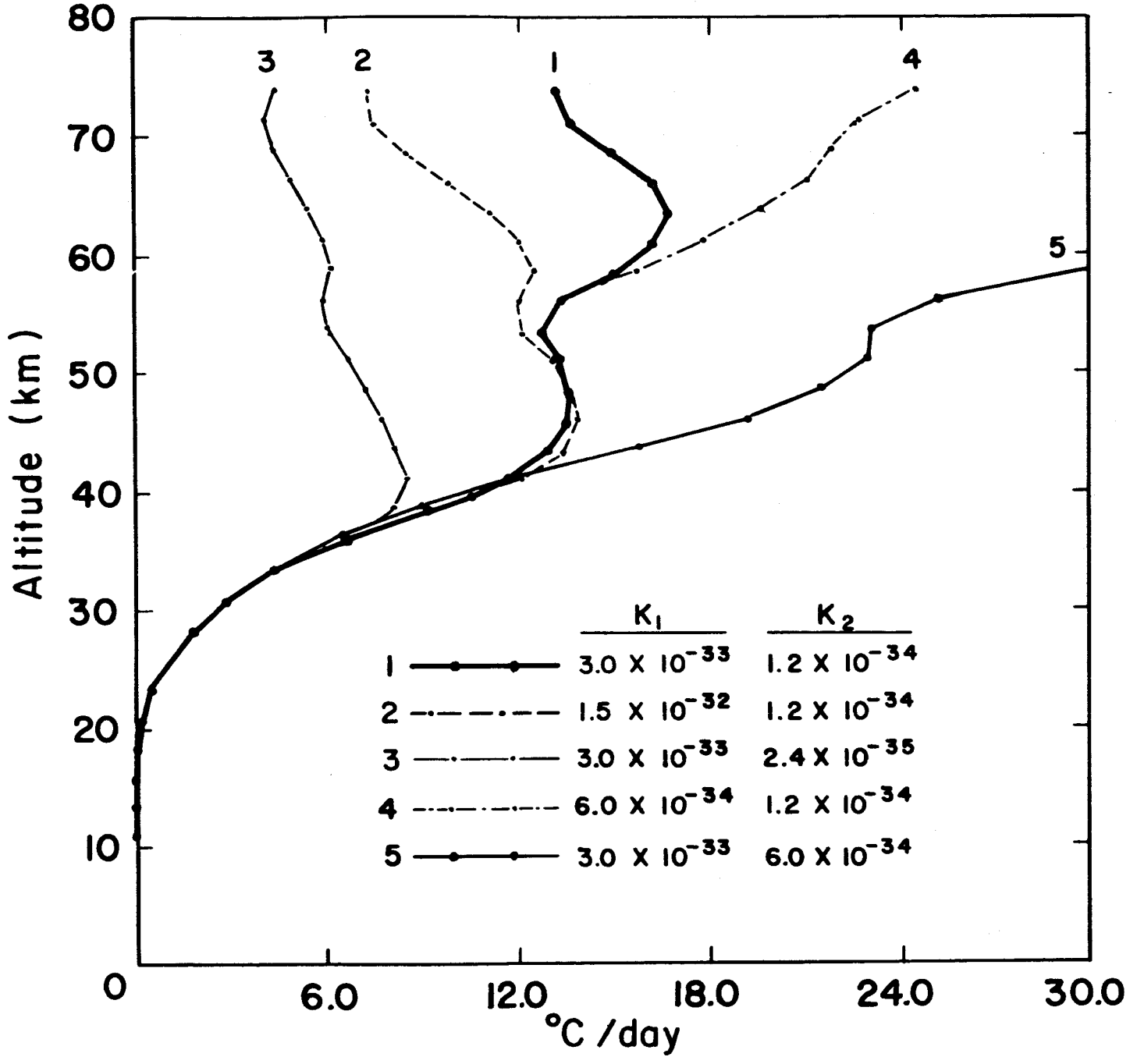
80
70
60
50
40
30
20
10
0
Altitude (km)
6.0
12.0
18.0
24.0
30.0
°C /day
1
2
3
4
5
K1
K2
1 3.0 X 10-33 1.2 X 10-34
2 1.5 X 10-32 1.2 X 10-34
3 3.0 X 10-33 2.4 X 10-35
4 6.0 X 10-34 1.2 X 10-34
5 3.0 X 10-33 6.0 X 10-34

Fig. A-2